© 2022. Published by The Company of Biologists Ltd | Development (2022) 149, dev200795. doi:10.1242/dev.200795

RESEARCH ARTICLE

The CRL4 E3 ligase Mahjong/DCAF1 controls cell competition through the transcription factor Xrp1, independently of polarity genes

Amit Kumar and Nicholas E. Baker*

ABSTRACT

Cell competition, the elimination of cells surrounded by more fit neighbors, is proposed to suppress tumorigenesis. Mahjong (Mahj), a ubiquitin E3 ligase substrate receptor, has been thought to mediate competition of cells mutated for *lethal giant larvae* (*lgl*), a neoplastic tumor suppressor that defines apical-basal polarity of epithelial cells. Here, we show that *Drosophila* cells mutated for *mahjong*, but not for *lgl* [*l(2)gl*], are competed because they express the bZip-domain transcription factor *Xrp1*, already known to eliminate cells heterozygous for ribosomal protein gene mutations (*Rp*/+ cells). *Xrp1* expression in *mahj* mutant cells results in activation of JNK signaling, autophagosome accumulation, eIF2α phosphorylation and lower translation, just as in *Rp*/+ cells. Cells mutated for *damage DNA binding-protein 1* (*ddb1*; *pic*) or *cullin 4* (*cul4*), which encode E3 ligase partners of Mahj, also display *Xrp1*-dependent phenotypes, as does knockdown of proteasome subunits. Our data suggest a new model of *mahj*-mediated cell competition that is independent of apical-basal polarity and couples Xrp1 to protein turnover.

KEY WORDS: Cell competition, Xrp1, Mahjong, DCAF1, Cullin 4, DDB1, Lethal giant larvae

INTRODUCTION

Cell competition, which is the elimination of, in most cases, slower-growing cells by faster-growing cells in mosaics, is important for precise development, regeneration and physiological maintenance (Clavería and Torres, 2016; Nagata and Igaki, 2018; Baker, 2020; Morata, 2021; Parker et al., 2021). Cell competition was first recognized in *Drosophila* in the case of cells lacking one copy of ribosomal protein genes (*Rp*/+). These mutants, which are known as '*Minutes*' because of their thin body bristles, also display slow growth (Bridges and Morgan, 1923; Lambertsson, 1998). *Minute* mutant cells are eliminated from mosaics with wild-type cells by caspase-dependent cell death (Morata and Ripoll, 1975; Simpson and Morata, 1981; Moreno et al., 2002; Li and Baker, 2007; Kale et al., 2015). Super-competition, the name given to the process of eliminating wild-type cells, happens in mosaics with faster-growing Myc- or Yorkie (Yki)-expressing cells (de la Cova et al., 2004; Moreno and Basler, 2004; Tyler et al., 2007; Neto-Silva et al., 2010). Considered together, cell competition and super-competition suggest that comparison of cellular fitness leads to cell competition. Because the mammalian homologs of Myc and Yki are proto-oncogenes (Dang, 2012; Moroishi et al., 2015), it has been suggested that super-competition might contribute to tumor expansion, as several recent studies have confirmed (Suijkerbuijk et al., 2016; Di Giacomo et al., 2017; Patel et al., 2017; Liu et al., 2019; Madan et al., 2019; Moya et al., 2019).

Cell competition may also be tumor suppressive. Global loss of apico-basal polarity genes such as *lgl* [*l(2)gl)*] or *scribble* (*scrib*) leads to polarity-deficient neoplasia of *Drosophila* imaginal discs (Bilder et al., 2000; Bilder and Perrimon, 2000; Humbert et al., 2003), but clones of *lgl* or *scrib* cells are eliminated from mosaics (Igaki et al., 2006; Froldi et al., 2010; Menendez et al., 2010; Tamori et al., 2010; Chen et al., 2012). These *lgl* or *scrib* mutant clones do not form tumors unless cell competition is blocked and mutant cells remain in the epithelium (Menendez et al., 2010; Chen et al., 2012; Khan et al., 2013).

Competition of *Rp*/+ mutant cells might also serve a tumor-surveillance role. Rp genes are spread throughout the genome (Uechi et al., 2001; Marygold et al., 2007), and it has been shown they can serve as sensors for aneuploidy, leading to elimination of aneuploid cells containing monosomies that affect Rp gene dose (Ji et al., 2021). Mutants with disrupted cell competition accumulate aneuploid cells (Ji et al., 2021). These would be expected to be tumorigenic in mammals, where aneuploidy is associated with tumorigenesis (Ben-David and Amon, 2020; Molina et al., 2021; Li and Zhu, 2022). Competition of *Rp*/+ cells depends on the *Drosophila* bZip AT-hook domain transcription factor *Xrp1* (Lee et al., 2016; Baillon et al., 2018; Lee et al., 2018). The *Xrp1* expression induced in *Rp*/+ imaginal discs is also responsible for most of their altered gene expression, their slow growth and their reduced translation, in addition to their propensity to be eliminated by cell competition (Lee et al., 2018). *Xrp1* is also expressed in the DNA damage response, where its transcription is *p53* dependent (Brodsky et al., 2004; Akdemir et al., 2007). *Xrp1* induction in *Rp*/+ cells is independent of *p53* but dependent on a particular Rp protein, RpS12, which is thought to play a role in signaling the defect in ribosome biogenesis (Kale et al., 2015; Kale et al., 2018; Lee et al., 2018; Ji et al., 2019).

The tumor-suppressive cell competition of polarity gene mutant cells has been proposed to go through Mahjong (Mahj) (Tamori et al., 2010), a CRL4 E3 ubiquitin ligase (Ly et al., 2019). Mahj physically interacts with Lgl, and its overexpression in *lgl* mutant clones suppresses their elimination from mosaic tissues (Tamori et al., 2010). Interestingly, *mahj* knockdown in MDCK cell cultures also leads to their elimination by co-cultured normal MDCK cells, suggesting a cell competition mechanism that is conserved between *Drosophila* and mammalian cells (Tamori et al., 2010). The mammalian homolog of *mahj*, known as DDB1-Cul4-associated

Department of Genetics, Albert Einstein College of Medicine, 1300 Morris Park Avenue, Bronx, NY 10461, USA.

*Author for correspondence (nicholas.baker@einsteinmed.edu)

N.E.B., 0000-0002-4250-3488

Handling Editor: Thomas Lecuit
Received 28 March 2022; Accepted 10 October 2022

Development (2022) 149, dev200795. doi:10.1242/dev.200795

factor 1 (DCAF1) or human immunodeficiency virus type 1 accessory protein Vpr-binding protein (VprBP), is important for G2 cell cycle arrest and virus replication after HIV1 infection (Le Rouzic et al., 2007; Tan et al., 2007). *Dcaf1* is required for mouse embryogenesis and its knockdown affects cell proliferation, cell cycle and cell survival in multiple cell types (McCall et al., 2008; Guo et al., 2016). *Dcaf1* interacts with the Hippo pathway and its knockdown also stabilizes p53 (Li et al., 2014; Ly et al., 2019; Han et al., 2020), but there has been no report of Dcaf1/VprBP affecting epithelial cell polarity in mammals.

In *Drosophila,* the overall transcriptional signature of *mahj* mutant wing discs is unexpectedly similar to that of *Rp*/+ mutants, including upregulation of *Xrp1* mRNA (Kucinski et al., 2017). Because *mahj* and *Rp*/+ cells were thought to represent distinct mechanisms of cell competition, this finding suggested a gene expression signature common to cells targeted by cell competition (Kucinski et al., 2017). Besides transcription, other similarities have been reported between *mahj* and *Rp*/+ mutant cells, including autophagosome accumulation and evidence of proteotoxic stress (Nagata et al., 2019; Baumgartner et al., 2021).

Here, we show that *mahj* mutant cells trigger cell competition through an *Xrp1*-dependent pathway like that in *Rp*/+ cells, and distinct from cell competition of *lgl* or *scrib* clones, which do not express or depend on *Xrp1* function for elimination. *Xrp1* expression also makes *mahj* mutant cells phenotypically like *Rp*/+ cells, that is, results in '*Minute*-like' thin thoracic bristles, slow growth, reduced translation, altered autophagy and increased JNK signaling. Regulation of Xrp1 by *mahj* likely requires its E3 ligase activity, depending on DNA Damage Binding Protein 1 (Ddb1) and Cullin 4 (Cul4). These results show that *mahj* mutant cells suffer cell competition because of a transcriptional response to altered ubiquitinylation mediated by Xrp1 and therefore resembling *Rp*/+ mutant cells. This seems unrelated to elimination of *scrib* or *lgl* mutant cells – the polarity-defective cells. Thus, loss of *mahj* function is an additional genotype triggering elimination by the Xrp1-dependent pathway that also removes Minute cells, not the mechanism for eliminating tumorigenic polarity-deficient cells.

RESULTS

Xrp1-dependent cell competition and *Minute*-like phenotypes of *mahj* mutant cells

Because *Xrp1* mRNA is elevated in *mahj* mutant wing discs (Kucinski et al., 2017), we examined Xrp1 protein expression and Xrp1 function in clones of cells undergoing cell competition due to loss of *mahj*. First, loss-of-function clones of $mahj^{1}$ allele were created; these are known to be outcompeted when next to control (*mahj*/+ or +/+) cells (Tamori et al., 2010). Xrp1 protein expression was examined making use of an allele tagged with HA at the endogenous *Xrp1* locus (Blanco et al., 2020). Xrp1-HA protein was undetectable in wild-type cells but clearly expressed in $mahj^{1}$ loss-of-function clones in the wing discs (Fig. 1A,A′). We also knocked down *mahj* through expression of dsRNA in the posterior wing compartment using en-Gal4. *mahj* knockdown in posterior compartments also resulted in Xrp1-HA protein expression (Fig. 1B,B′). This indicates that cell competition is not required for Xrp1 expression, as all the posterior compartment cells are depleted of *mahj*. Interestingly, *mahj* knockdown also reduced the relative size of the posterior compartments, a result that was variable but statistically significant (Fig. S1A-C). The reduction in posterior compartment size suggests *mahj* knockdown impacts cellular growth regulation. We made multiple attempts to assess whether *Xrp1* is required for the reduced compartmental growth that results from *mahj* depletion in wing disc compartments, but so far it has not been possible to obtain larvae of these *mahj Xrp1* co-depletion genotypes.

To determine the functional significance of Xrp1 protein expression in *mahj* mutant cells, the size of $mahj^{1}$ mutant clones was compared with parallel $mahj^{1}$ clones expressing *Xrp1* RNAi, and we also measured apoptosis in these clones. *Xrp1* knockdown rescued $mahj^{1}$ clone size significantly and reduced the cell death that was otherwise seen at the boundaries of *mahj* mutant clones with wild-type areas (Fig. 1C-G). The functional requirement for *Xrp1* was further confirmed by making flip-out clones that expressed *mahj* dsRNA, in comparison with clones expressing both *mahj* dsRNA and *Xrp1* dsRNA. In this case also, clone size and boundary cell death were significantly rescued by *Xrp1* knockdown (Fig. S1D-H). Notably, we occasionally found accumulation of some dying cells accumulating within the *mahj Xrp1* double knockdown clones (Fig. S1F,F′, cyan arrowhead). It is important to note that, not only do the similar phenotypes of *mahj* mutant clones and clones expressing *mahj* dsRNA confirm the specificity for *mahj* loss of function and argue against any off-target effect or passenger mutation causing the cell competition, but the rescue of *mahj* phenotypes using distinct *Xrp1* dsRNAs also confirms the specificity of the *Xrp1* knockdown results.

Finally, *Xrp1* loss-of-function clones were made in a global *mahj* mutant background. Reminiscent of FRT82 control clones and their twin spots (Fig. 1H), *Xrp1* loss of function clones grow similarly to twin-spot controls in an otherwise wild-type context (Lee et al., 2018). By contrast, *Xrp1* mutant clones were enlarged in *mahj* mutants and the twin spots almost eliminated (Fig. 1I,J). This suggests that *Xrp1* was sufficient to induce cell competition between *mahj* mutant cells based on Xrp1 expression. Clearly, *mahj* mutant cells expressing two wild-type copies of *Xrp1* were disadvantaged compared with *mahj* mutant cells that were also mutant for *Xrp1*.

Because we found that *mahj* mutant cells resembled *Rp*/+ cells in their *Xrp1*-dependent cell competition, and in reduced growth rate (Fig. 1C-J), we wondered whether *mahj* loss of function would affect bristle size, as *Rp* mutations do (Bridges and Morgan, 1923). As predicted, expression of *mahj* dsRNA specifically in bristle primordia resulted in small and thin bristles, similar to *Rp*/+ mutants (Fig. 1K,L). Although expression of *Xrp1* dsRNA by itself had no effect on bristles (Fig. 1N), the *mahj* knockdown phenotype was partially rescued upon co-expression of *Xrp1* ds RNA (Fig. 1M,O), illustrating another similarity between *mahj* and *Rp*/+ phenotypes.

Xrp1-dependent defects in *mahj* mutant cells

mahj mutant cells are reported to exhibit multiple abnormalities that are also seen in *Rp*/+ mutant cells (Kucinski et al., 2017; Nagata et al., 2019), in which case they are *Xrp1* dependent (Lee et al., 2018). First, JNK signaling is activated in and required for the competitive cell death of *mahj* mutant cells (Tamori et al., 2010). Elevated JNK activity is *Xrp1* dependent in *Rp*/+ mutant cells (Lee et al., 2018). We found that, similarly, JNK hyperactivity disappeared from *mahj* mutant cells after *Xrp1* knockdown (Fig. 2A-B″, Fig. S2A). Second, autophagosomes accumulate in both *mahj* mutant clones and *Rp*/+ mutant cells (Nagata et al., 2019; Baumgartner et al., 2021). Autophagosome accumulation is *Xrp1* dependent in *Rp*/+ mutant cells (Langton et al., 2021; Kiparaki et al., 2022). Autophagosomes are believed to accumulate because of reduced autophagic flux, although there is disagreement about whether autophagy is detrimental or protective for *Rp*/+ cells(Nagata et al., 2019; Baumgartner et al., 2021). Using lysotracker dye accumulation as a marker for autophagosomes

Development (2022) 149, dev200795. doi:10.1242/dev.200795

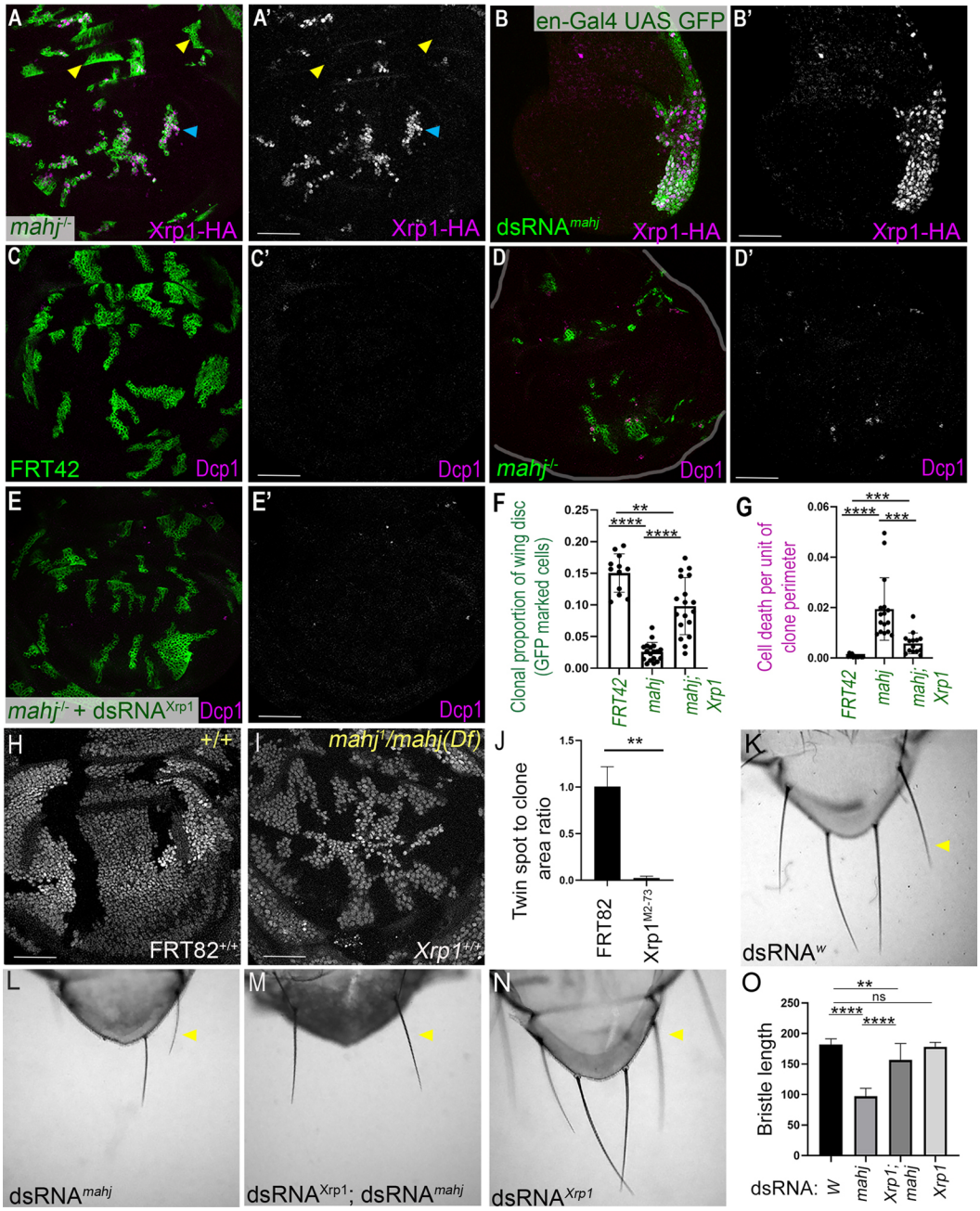

Fig. 1. *Xrp1*-dependent cell competition after *mahj* loss. (A,A′) Wing disc with *mahj* mutant clones marked by GFP expression (green, tub-Gal4>UAS-GFP). Xrp1-HA expression is shown in magenta. Expression of Xrp1-HA is present in many *mahj* clones and is more common in the clones of pouch domain (cyan arrowhead). Clones in the wing hinge domain (yellow arrowhead) do not always express Xrp1-HA. Cell competition is known to be more severe in the wing pouch than the wing hinge (Khan et al., 2013). *n*=7. (B,B′) Expression of Xrp1-HA (magenta) is observed upon *mahj* RNAi in the posterior compartment (green, engrailed driver, *n*=7). All cells display Xrp1-HA expression and the posterior compartment is significantly smaller than the anterior. (C-E′) Wing discs with mosaic clones marked in green for FRT42 control (C,C′), *mahj* mutant (D,D′) and *Xrp1* RNAi expressing *mahj* mutant (E,E′) cells (driven by tub-Gal4E). Dying cells were labelled using anti-Dcp1 staining (magenta). (D,D′) *mahj* mutant clones are smaller than control clones and display cell death at clone borders (compare C with D). (E,E′) Knockdown of *Xrp1* in *mahj* clones rescued clone size and decreased cell death at the clone border. *n*=13, 16, 14 for genotypes in C, D and E, respectively. (F) Quantification of clone size in the three genotypes presented in C-E′. (G) Quantification of cell death in the three genotypes presented in C-E′. Each dot in F and G represents data from an individual wing disc. (H) FRT82 control clones (black) and their reciprocal twin spots in wild-type wing disc (white, *n*=6). (I) In the *mahj* mutant background, clones lacking *Xrp1* (black) survived but the reciprocal twin spots with two copies of wild-type Xrp1 were almost eliminated (white, *n*=6). (J) Quantification of twin spot to clone ratio in H and I genotypes (in the log scale). (K-N) Thoracic bristles with knockdown of *white* (K), *mahj* (L), *mahj* plus *Xrp1* (M) and *Xrp1* (N) by expression of corresponding dsRNA driven by G109-68-Gal4. Arrowheads indicate anterior scutellar bristles. (O) Quantification of anterior scutellar bristle length in genotypes shown in K-N. The reduction in bristle size in response to *mahj* knockdown is mostly Xrp1 dependent. *n* =13, 19, 26 and 15 for K-N, respectively. ****P<0.0001, ***$P\leq$0.0005, **$P\leq$0.0025; ns, not significant (unpaired *t*-test for F, G, O; Mann–Whitney test for J). Data are mean±s.d. Scale bars: 50 µm.

(Nagata et al., 2019; Recasens-Alvarez et al., 2021), we confirmed accumulation in *mahj* mutant discs, which was *Xrp1* dependent (Fig. 2C-E, Fig. S2B). Third, some authors have reported lower general translation levels in *mahj* mutant cells (Nagata et al., 2019), although this has not been observed by others (Baumgartner et al., 2021). Reduced translation is also a feature of *Rp*/+ mutant cells,

Development (2022) 149, dev200795. doi:10.1242/dev.200795

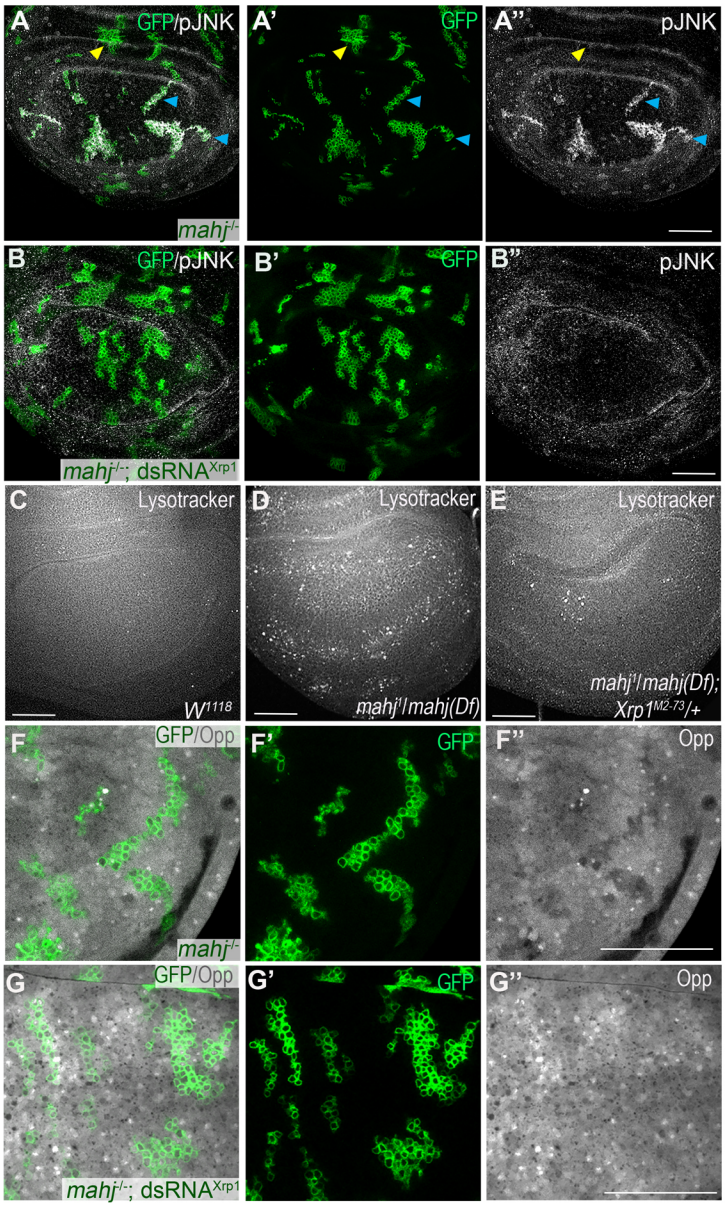

Fig. 2. *mahj* mutant cells display a *Rp*/+-like phenotype under the regulation of *Xrp1*. (A-B″) Loss-of-function clones of *mahj* marked (green, tub-Gal4>UAS-GFP) stained using anti-pJNK (gray). (A-A″) There is a higher level of pJNK in *mahj* clones compared with adjacent wild-type cells, especially in the clones of pouch domain (cyan and yellow arrowheads mark clones of the pouch and hinge domain, respectively, *n*=7). (B-B″) *Xrp1* knockdown abolished higher levels of JNK phosphorylation (*n*=7). (C-E) Lysotracker staining. (C) Wild type (*n*=12), (D) *mahj* (shows elevated lysotracker; *n*=12) and (E) *mahj; Xrp1*/+ wing discs (*n*=10). Lysotracker dye is restored to almost control levels in E. (F-G″) Translation levels (OPP incorporation) in *mahj* mutant clones. (F-F″) *mahj* clones (green) display reduced global translation (*n*=7). (G-G″) Global translation rate was restored in *mahj* clones in which *Xrp1* is knocked down (*n*=5). Scale bars: 50 µm.

where it is *Xrp1* dependent (Lee et al., 2018). Using accumulation of OPP (O-propargyl-puromycin), an alkyne analog of puromycin, to measure total cellular translation (Lee et al., 2018), we confirmed that *mahj* mutant clones displayed lower translation than wild-type cells (Fig. 2F-F″). The difference was abolished by *Xrp1* knockdown, indicating that overall translation is reduced by *Xrp1* in both *Rp*/+ and *mahj* mutant cells (Fig. 2G-G″). Overall, multiple cellular defects in *mahj* mutant cells were found to be *Xrp1* dependent.

Xrp1 induction by a novel mechanism in *mahj* mutant cells

The expression of Xrp1 protein, which is very low in wild-type imaginal discs, is known to be induced through multiple distinct mechanisms. First, *Xrp1* is the major transcriptional target of *p53* after DNA damage (Brodsky et al., 2004; Akdemir et al., 2007). Second, in *Rp*/+ mutants, *Xrp1* expression depends on *rpS12*, not *p53* (Lee et al., 2018; Ji et al., 2019). Finally, Xrp1 protein expression can be induced by eIF2α phosphorylation (Brown et al., 2021; Langton et al., 2021; Ochi et al., 2021; Kiparaki et al., 2022). eIF2α phosphorylation commonly occurs as a result of ER stress and results in the overall reduction of CAP-dependent translation initiation, while favoring the translation of some transcripts (Ryoo and Vasudevan, 2017; Wek, 2018).

To assess the role of *p53*, we knocked *mahj* down in posterior wing compartments, and observed the same level of Xrp1-HA expression even when dominant-negative *p53* (*p53*-DN) was co-expressed (Fig. 3A-B′, Fig. S3A). We also compared expression of a P53 reporter, rpr-150 lacZ (Brodsky et al., 2000), upon *mahj* knockdown and observed no change. This indicates that loss of *mahj* does not increase *p53* activity, which should activate this reporter (Fig. S3B,B′). Finally, *p53* dsRNA failed to rescue competitive elimination of *mahj* mutant clones (Fig. S3E-G), although p53 dsRNA was sufficient to prevent cell death induced by irradiation (Fig. S3C-D).

To assess the role of Rps12, Xrp1-HA protein expression in *mahj* mutant clones was assessed in the background of the $rpS12^{G97D}$, the *rpS12* mutation that prevents *Xrp1* induction in *Rp*/+ cells

Development (2022) 149, dev200795. doi:10.1242/dev.200795

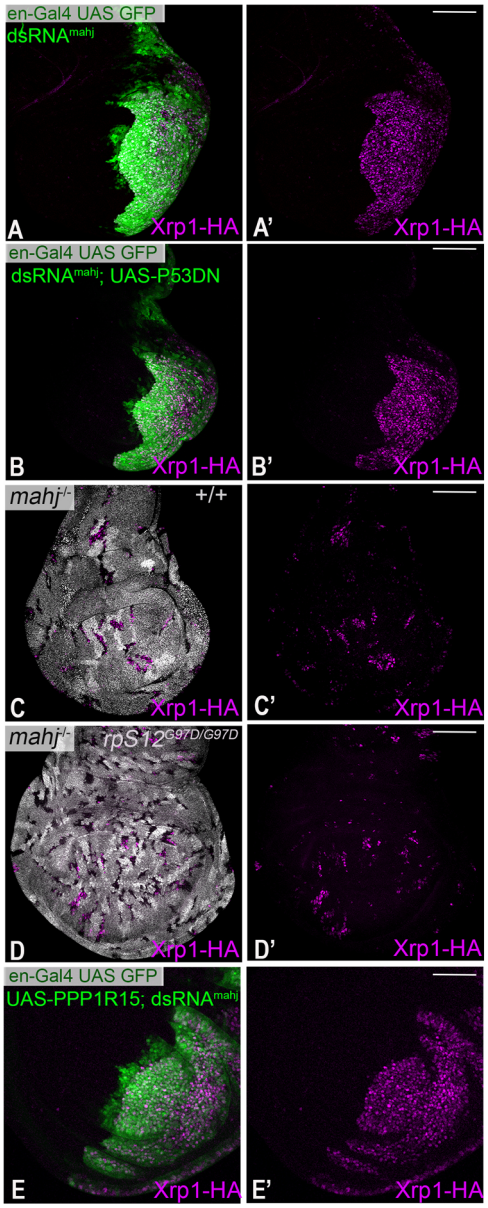

Fig. 3. *mahj* mutant cells express Xrp1 independently of known regulators. (A-B′) Wing discs with knockdown of *mahj* in the posterior compartment (green) and Xrp1-HA expression (magenta, A′). (A,A′) *mahj* knockdown induced Xrp1-HA. (B,B′) Simultaneous expression of UAS-*p53* DN had no effect on Xrp1-HA expression (compare A′ with B′). *n*=9 and 10 for A and B, respectively. (C-D′) Wing discs with *mahj* mutant clones (black) and reciprocal twin spot controls (white); expression of Xrp1-HA in magenta. (C,C′) Xrp1-HA was induced in *mahj* mutant clones. (D,D′) Xrp1-HA expression was also comparable in *mahj* clones in the *rpS12*^{G97D} background. *n*=4 for C and D. (E,E′) A wing disc with knockdown of *mahj* in the posterior compartment with simultaneous expression of UAS-*PP1R15*. The expression level of Xrp1-HA (E′) is comparable with control (see Fig. S4H for quantification and *n*). Scale bars: 50 µm.

(Kale et al., 2018; Lee et al., 2018). Xrp1-HA protein expression in *mahj* mutant clones was unaffected (Fig. 3C-D′, Fig. S4A), as was their growth and survival, indicating that *rpS12* was not required for *mahj* mediated cell competition (Fig. S4B-D). Moreover, an *Xrp1*-LacZ enhancer trap was unaffected by *mahj* knockdown in posterior wing compartments (Fig. S4E,E′), although RpS12 regulates this enhancer trap in *Rp*/+ cells (Lee et al., 2018; Ji et al., 2019). Because *Xrp1* mRNA levels are elevated in *mahj* mutants (Kucinski et al., 2017), this suggests the *Xrp1*-LacZ enhancer trap may not report all aspects of *Xrp1* mRNA regulation.

We found that *mahj* knockdown resulted in higher eIF2α phosphorylation (Fig. S4F-G). eIF2α is also phosphorylated in *Rp*/+ cells, and is responsible for their reduced overall translation rate (Baumgartner et al., 2021; Langton et al., 2021; Ochi et al., 2021; Recasens-Alvarez et al., 2021; Kiparaki et al., 2022). As for *Rp*/+ cells (Kiparaki et al., 2022), co-expression of the eIF2α phosphatase *PPP1R15* had no effect on Xrp1-HA levels induced by *mahj* dsRNA, indicating that eIF2 α phosphorylation was not required for Xrp1 protein expression caused by *mahj* depletion (Fig. 3E, Fig. S4H). Overall, none of the currently known mechanisms explains induction of *Xrp1* upon *mahj* knockdown, suggesting an additional way to induce Xrp1 and launch cell competition in *mahj* mutant cells.

The CRL4M^{Mahj} complex regulates Xrp1 expression and cell competition

We explored whether *mahj* regulates Xrp1 protein expression and cell competition, through its ubiquitin ligase function. Cullin Ring Ubiquitin ligases (CRL) are the largest family of E3 ubiquitin ligases (Hershko and Ciechanover, 1998; Sang et al., 2015). Cullins act as scaffolds to link a Ring-box protein required for interactions with an E2 ubiquitin ligase with an adapter protein that recruits substrates and determines the substrate specificity of ubiquitylation (Petroski and Deshaies, 2005; Angers et al., 2006). Mahj is such a substrate adapter, binding to Cul4 through DDB1 to constitute the CRL4 (Ly et al., 2019). We found that knockdown of either *cul4* or *ddb1* resulted in Xrp1 protein expression in wing discs (Fig. 4A-B′). Xrp1 protein expression was also observed upon knockdown of *Roc1a* (Fig. S5A,A′), which is responsible for CRL4 interaction with the E2 ligase (Angers et al., 2006). Cul4 function requires neddylation with Nedd8 (Pan et al., 2004). Mutation of the neddylation sites results in a dominant-negative Cul4 molecule (Lin et al., 2009). Over-expression of dominant-negative Cul4 also resulted in Xrp1 protein expression in wing discs (Fig. 4C,C′). Finally, as expected if perturbation in ubiquitin-mediated protein turnover is responsible for Xrp1 protein expression in *mahj* mutants, Xrp1 protein expression was also observed upon knockdown of different proteasome subunits (Fig. 4D,D′, Fig. S5B-C′). If *mahj* mutants lead to cell competition by affecting ubiquitin-dependent protein turnover, we would expect that knocking down the partners of Mahj in the CRL4 complex would also lead to cell competition. Consistent with this notion, knockdown of *cul4* is known to result in poor clone survival (Tare et al., 2016). Here, we made *ddb1* knockdown clones by expressing *ddb1* RNAi in actin Gal4 flip-out clones. 48 h after induction, these clones displayed extensive cell death both at the boundaries with wild-type cells and within the clones themselves (Fig. 5A-B′). No *ddb1* knockdown clones could be detected 72 h after clone induction (Fig. 5G). Significantly, simultaneous knockdown of *Xrp1* within the clones dramatically reduced cell death both at the clone boundary and within clones (Fig. 5C-E), and allowed these clones to survive for 72 h (Fig. 5F-I). Similar to *ddb1* knockdown clones, expression of *cul4* RNAi in actin-Gal4 flip-out clones for 48 h also resulted in cell death both within clones as well as at clone borders, dependent on *Xrp1* in most wing discs (*n*=8/10, Fig. S6A-B′,D-E). A few discs did not show rescue of cell death (*n*=2/10, Fig. S6C,C′). Additionally, like *mahj* knockdown, expression of *cul4* RNAi resulted in phosphorylation of eIF2α in an *Xrp1*-dependent manner (Fig. 5J-K′).

Overall, these findings show that *ddb1* and *cul4* loss of function result in Xrp1 protein expression and Xrp1-dependent clone

Development (2022) 149, dev200795. doi:10.1242/dev.200795

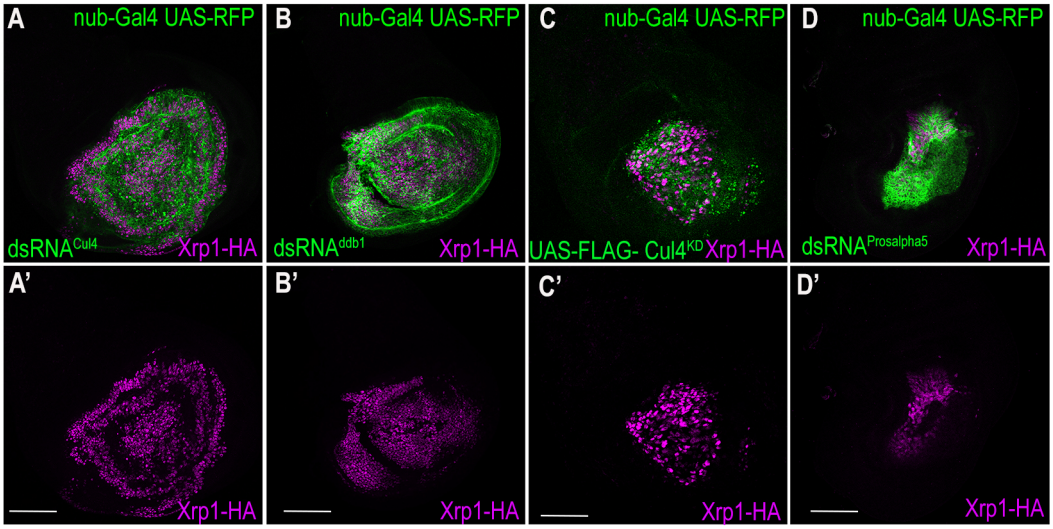

Fig. 4. Xrp1 expression in *mahj* is E3 ligase dependent. (A-D′) Wing discs with RFP (green) and the indicated transgenes expressed in the wing pouch domain with nubbin-Gal4. Xrp1-HA expression is in magenta. (A,A′) *cul4* knockdown activates Xrp1-HA (*n*=6). (B,B′) *ddb1* knockdown activates Xrp1-HA (*n*=11). (C,C′) *cul4* dominant-negative expression activates Xrp1-HA (*n*=8). (D,D′) Knockdown of proteasome subunit *Prosα5* activates Xrp1-HA (*n*=8). Scale bars: 50 µm.

elimination similar to that seen with loss of *mahj*. This strongly suggests that *mahj* regulates cell competition through CRL4-dependent ubiquitylation of a protein that would otherwise promote Xrp1 expression. It is interesting that *ddb1* mutants also show '*Minute*'-like bristles (He et al., 2006), a further connection between the ubiquitin ligase function of *mahj* and the *Minute* phenotype caused by *Rp*/+ genotypes. It is possible that *ddb1* and *cul4* loss of function also cause cell-autonomous cell death due to other survival roles of these genes.

The Mahj substrate Warts is dispensable for Xrp1 expression

In neural stem cells, Mahj recruits Warts for CRL4-dependent ubiquitylation (Ly et al., 2019). Warts (Wts), a serine threonine kinase, is a member of the Hippo pathway that phosphorylates and inhibits the transcription co-activator Yorkie (Yki), thereby inhibiting growth (Justice et al., 1995; Wu et al., 2003; Huang et al., 2005; Dong et al., 2007; Hao et al., 2008). Because Yki affects cellular growth and differences in Yki activity can trigger competition between cells (Tyler et al., 2007; Neto-Silva et al., 2010), we wondered whether Warts could be the Mahj target regulating *Xrp1* expression and cell competition in *mahj* mutant cells. To check how Warts affects *mahj* clones in wing discs, we first examined Hippo signaling reporters after knockdown of *mahj*. LacZ reporters of *ex*, *fj* and *diap*, which are sensitive to Hippo signaling (Wu et al., 2003; Cho et al., 2006; Hamaratoglu et al., 2006; Tyler and Baker, 2007; Wang and Baker, 2015), were each downregulated in posterior compartments upon *mahj* knockdown, consistent with reduced Yki activity (Fig. 6A-C′), and as expected based on the neural stem cell findings (Ly et al., 2019). However, no changes in the reporters were observed upon *mahj* overexpression (Fig. S7A-B′), suggesting that *mahj* is required but not sufficient to regulate Wts in the wing disc. Interestingly, *wts* mutant clones also displayed higher translation (Fig. 6D,D′), as did overexpression of Yki or of its miRNA target Bantam [Fig. S7C-D′, also recently reported by another group (Nagata et al., 2022)], which would be consistent with the Hippo pathway affecting Xrp1. To test whether Warts stabilization is the mechanism whereby *mahj* regulates Xrp1 and translation (Ly et al., 2019), Wts was overexpressed in the wing discs.

Wts overexpression led to the expected reduction in size of the wing pouch (Lai et al., 2005), but no Xrp1-HA protein expression was observed (Fig. 6E-F′). Similar results were obtained after overexpression of hippo (*hpo*), which encodes a serine threonine kinase that phosphorylates Warts and positively regulates Warts activity (Pantalacci et al., 2003; Wu et al., 2003). Hpo overexpression also greatly reduces growth of wing disc cells (Huang et al., 2005; Tyler and Baker, 2007), and led to a more severe reduction in size of the wing pouch than did Wts overexpression (Fig. 6F, Fig. S7F). Xrp1-HA protein expression was still not observed (Fig. S7E-F′). To investigate whether Hippo signaling might be necessary for Xrp1 expression, although not sufficient to induce it alone, we co-expressed *wts* RNAi and *mahj* RNAi, but observed no change in Xrp1 protein (Fig. 6G-H′, Fig. S7I). In the same way, Xrp1 protein expression was not changed in cells with knockdown for *mahj* and simultaneous overexpression of Yki (Fig. S7G-H′). These findings show that Hippo signaling and Yki activity levels do not contribute to Xrp1 expression in *mahj* mutant cells. Thus, although *mahj* did regulate Hippo signaling in wing discs, consistent with regulation of Warts stability, this did not seem to be the mechanism of Xrp1 protein expression in *mahj* mutant wing disc cells.

Polarity mutants display Xrp1-independent cell competition

Mahj came to the attention of the cell competition field as a binding partner of Lgl, proposed to mediate the competitive elimination of cells with *lgl* mutations and perhaps mutations for related cell polarity genes, including *scrib* (Tamori et al., 2010; Baker, 2011; Levayer and Moreno, 2013; Claveria and Torres, 2016). As we have found that *mahj* affects cell competition through *Xrp1* and therefore through a pathway broadly similar to that seen in *Rp*/+ cells, we expected that competitive elimination of *lgl* and *scrib* mutant clones would also be mediated by Xrp1. Contrary to this expectation, no Xrp1-HA expression was detected in *lgl* loss-of-function clones (Fig. 7A,A′). Moreover, there was no rescue in clone size or boundary cell death when *Xrp1* was knocked down in *lgl* mutant cells (Fig. 7B-D, Fig. S8A). We also found that *scrib* mutant clones were still eliminated in an *Xrp1* mutant background (Fig. 7E-G, Fig. S8B). Thus, *Xrp1* was not required

Development (2022) 149, dev200795. doi:10.1242/dev.200795

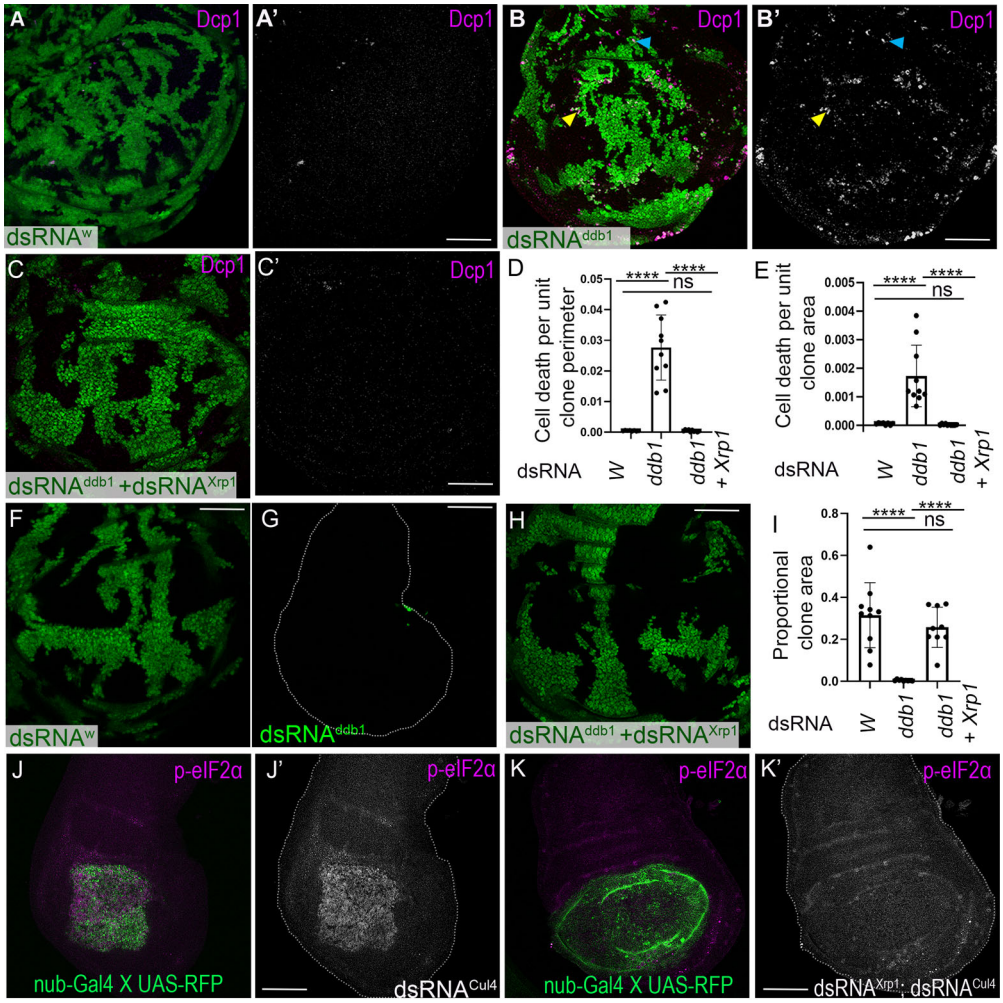

Fig. 5. Xrp1 regulates cellular phenotype upon knockdown of DDB1 and Cul4. (A-C′,F-H) Wing disc with flip-out knockdown clones (green) at 48 h (A-C′) or 72 h (F-H) after heat shock. (A,A′) Knockdown of *white* causes little cell death (magenta). (B,B′) Knockdown of *ddb1* induces cell death, especially near the boundaries with wild-type cells (magenta; cyan and yellow arrowheads mark dying cells within and at the clone boundary, respectively). (C,C′) Simultaneous *Xrp1* knockdown rescues apoptosis of *ddb1* knockdown cells (magenta). (D) Quantification of cell death as a function of clone perimeter. (E) Quantification of cell death as a function of clone area. $n \geq 8$ for genotypes shown in A-C′. (F) Wing disc with flip-out clones with *white* knockdown 72 h after induction (green). (G) Flip-out clones with *ddb1* knockdown are undetectable 72 h after induction (green). (H) Flip-out clones with *ddb1* knockdown are completely restored by simultaneous Xrp1 knockdown 72 h after induction (green). (I) Quantification of flip-out clones shown in F-H ($n \geq 9$). (J,J′) Wing disc with *nub*-Gal4 knockdown of *cul4* (green). eIF2α phosphorylation is increased (magenta) ($n=4$). (K,K′) Wing disc with *nub*-Gal4 knockdown of *cul4* and *Xrp1* (green) ($n=4$). eIF2α phosphorylation is not increased (magenta). ****$P<0.0001$; ns, not significant (Mann–Whitney test). Data are mean ±s.d. Each dot in a graph represent data from one wing disc in D, E and I. Scale bars: 50 µm.

for cell competition in these two polarity-defective mutant genotypes.

In many of our experiments where *mahj* was knocked down in posterior wing disc compartments, the A/P compartment boundary became markedly irregular, and sporadic loss of GFP expression was observed within the compartment. Double-labeling of every cell with DAPI confirmed that posterior compartments depleted for *mahj* often contain cells lacking GFP expression, something never seen in en-Gal4 UAS-GFP controls(Fig. 7H-I″). Such sporadic loss of marker expression is thought to reflect loss of heterozygosity reflecting genomic instability(Dekanty et al., 2012). Thus, *mahj* may have functions unrelated to epithelial cell polarity, including a contribution to genome stability yet to be fully elucidated in *Drosophila*.

DISCUSSION

In this research article, we explore the cell competition mechanisms of Mahj, a CRL4 ubiquitin ligase (Ly et al., 2019), the mutation of which triggers similar cellular effects to *Rp*/+ mutations, including similar changes in gene expression, global translation rates, JNK activity and autophagy, leading *mahj* cells to be eliminated by competition with wild-type cells, as *Rp*/+ cells are (Fig. 7J) (Tamori et al., 2010; Kucinski et al., 2017; Nagata et al., 2019). The basis of the similarity is that *mahj* and *Rp* loss of function both activate expression of *Xrp1*, the transcription factor that coordinates these effects (Figs 1,2). Unlike *Rp*/+ genotypes, which activate *Xrp1* through a *rpS12*-dependent mechanism (Lee et al., 2018; Ji et al., 2019), Mahj regulates Xrp1 most likely through its ubiquitin ligase activity, which depends on DDB1, Cul4 and Roc1a (Fig. 4, Fig. S5A,A′), although the specific ubiquitylated target has not yet been identified. We suggest that Xrp1 is likely to be activated by a protein, or proteins, that are normally degraded by Mahj-dependent ubiquitylation, because *Xrp1* is also activated by inhibition of the proteasome (Fig. 4D,D′, Fig. S5B-C′), which is expected to affect the degradation of ubiquitylated proteins, but not other functional

Development (2022) 149, dev200795. doi:10.1242/dev.200795

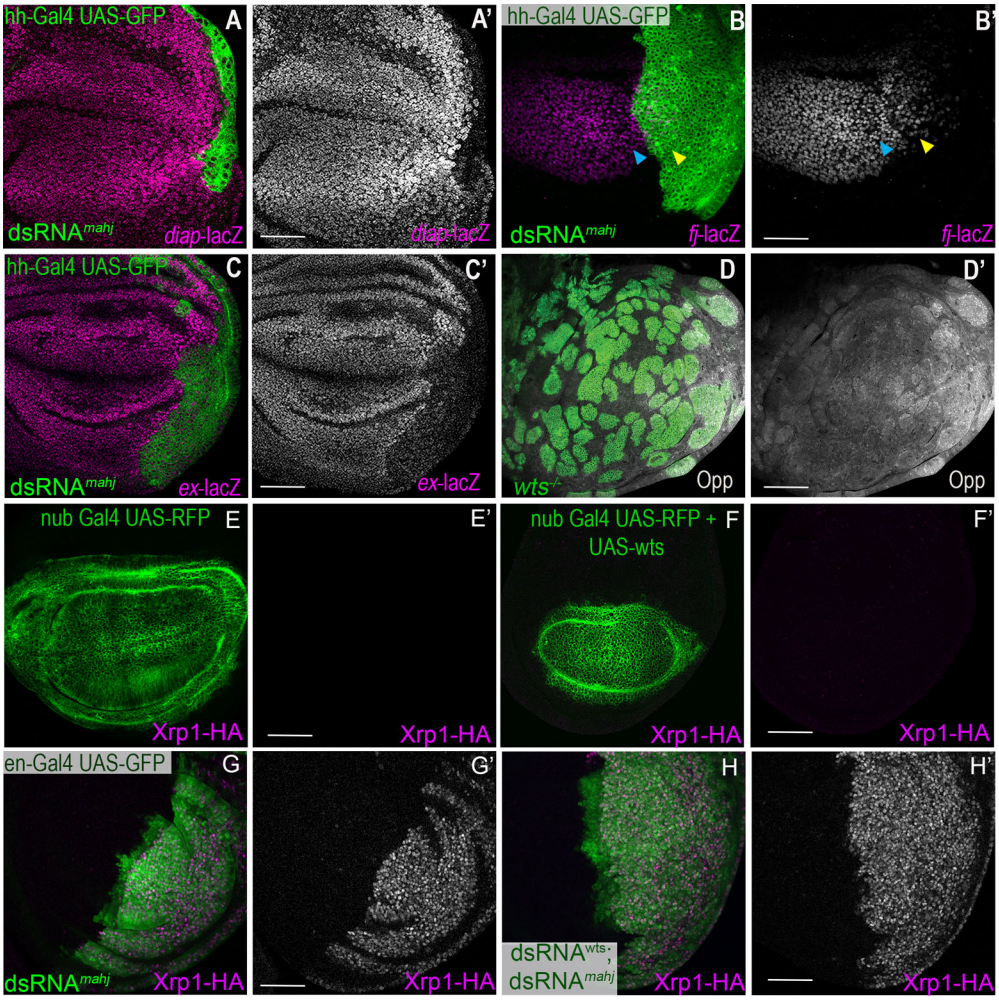

Fig. 6. *mahj* regulates SWH signaling without affecting cell competition. (A-C′) Wing disc with *mahj* knockdown in the posterior compartment (green); SWH reporters are in magenta. (A,A′) *diap*-LacZ is reduced by *mahj* knockdown (n=4). (B,B′) *fj*-LacZ is reduced by *mahj* knockdown (n=5). Blue and yellow arrowheads indicate anterior and posterior compartments, respectively. (C,C′) *ex*-LacZ is reduced by *mahj* knockdown (n=8). (D,D′) Translation rate (OPP labeling, gray) in wing disc with *wts* mutant clones (green) (n=8). There is more translation in *wts* clones. (E,E′) *nub*-Gal4 expression (green) did not induce Xrp1-HA in the wing pouch (magenta, n=8). (F,F′) *wts* overexpression using nub-Gal4 did not induce Xrp1-HA expression in the wing pouch (magenta, n=8). (G,G′) *mahj* knockdown induced Xrp1-HA in the posterior compartment (magenta, n=9). (H,H′) Xrp1-HA expression (magenta) continued in posterior compartments depleted of *mahj* and with co-expression of *wts* RNAi (green, n=8). Scale bars: 50 µm.

consequences of ubiquitylation. The relevant target does not seem to be Warts, despite the fact that levels of Warts and Hippo pathway activity also control cellular growth (Pantalacci et al., 2003; Udan et al., 2003; Wu et al., 2003; Huang et al., 2005) and global translation levels (Fig. 6D,D′, Fig. S7C-D′; Nagata et al., 2022), and can stimulate cell competition (Tyler et al., 2007; Neto-Silva et al., 2010). These studies support the notion that Xrp1 is a sensor of multiple cellular defects that cause cell competition, rather than that of a 'loser signature' common to distinct cell competition mechanisms. Another group has also reported that Xrp1 is required for cell competition of *mahj* mutant clones, but without the further analysis described here (Langton et al., 2021).

Mahj was previously thought to be responsible for the cell competition of cells mutated for *lgl* (Tamori et al., 2010; Baker, 2011; Levayer and Moreno, 2013), a gene that controls apical basal cell polarity (Bilder et al., 2000; Humbert et al., 2003). Mahj was originally linked to apical-basal polarity because of a physical interaction with Lgl, and because Mahj overexpression can rescue *lgl* mutant clones for elimination, suggesting that Mahj behaves as an intracellular signal transducer of *lgl* activity in cell competition (Tamori et al., 2010). As such, it was surprising when similar gene expression changes were observed in *mahj* mutant and *Rp* mutant wing discs, because these were assumed to reflect distinct cell competition pathways and suggested a common gene expression signature associated with competed cells (Kucinski et al., 2017). We show here, however, that neither *lgl* nor *scrib*, another related cell polarity gene (Bilder and Perrimon, 2000), affects cell competition by the same mechanism as *mahj*, because neither *lgl* nor *scrib* mutant cells express or require Xrp1 (Fig. 7, Fig. S8). Interestingly, several distinct pathways have recently been described to mediate the elimination of *scrib* mutant cells in competition with wild-type cells, and none of these pathways are shown to be required for the elimination of *Rp*/+ mutant cells (Vaughen and Igaki, 2016; Yamamoto et al., 2017). In addition, *mahj* loss by itself does not result in apical-basal polarity defects (Tamori et al., 2010), and its mammalian homolog is implicated in cell cycle regulation, genome integrity and *p53* activity (Hrecka et al., 2007; Cooper and Giancotti, 2014; Lubow and Collins, 2020). *Drosophila mahj*, which is an essential gene, regulates neural stem cell reactivation (Ly et al., 2019) and may have other roles in non-neuronal tissues, as suggested by defects observed when *mahj* is depleted in posterior wing compartments (Fig. 7H-I″). Accordingly, we conclude that *mahj* mutants affect cellular growth and cell competition in a manner unrelated to *lgl* and *scrib*, and that the functional relationship of *mahj* to apical-basal polarity pathways, should any exist, is unclear (Fig. 7J). The functional importance of physical interaction between Mahj and Lgl remains to be explored. It is known that *lgl* clones are rescued by reduced Hippo signaling (Menendez et al., 2010; Khan et al., 2013), although we did not detect reduced Hippo signaling after *mahj* overexpression in the absence of *lgl* mutations (Fig. S7A-B′).

Our studies provide further evidence for Xrp1 as an integrator of multiple seemingly independent cellular defects that each result in a

Development (2022) 149, dev200795. doi:10.1242/dev.200795

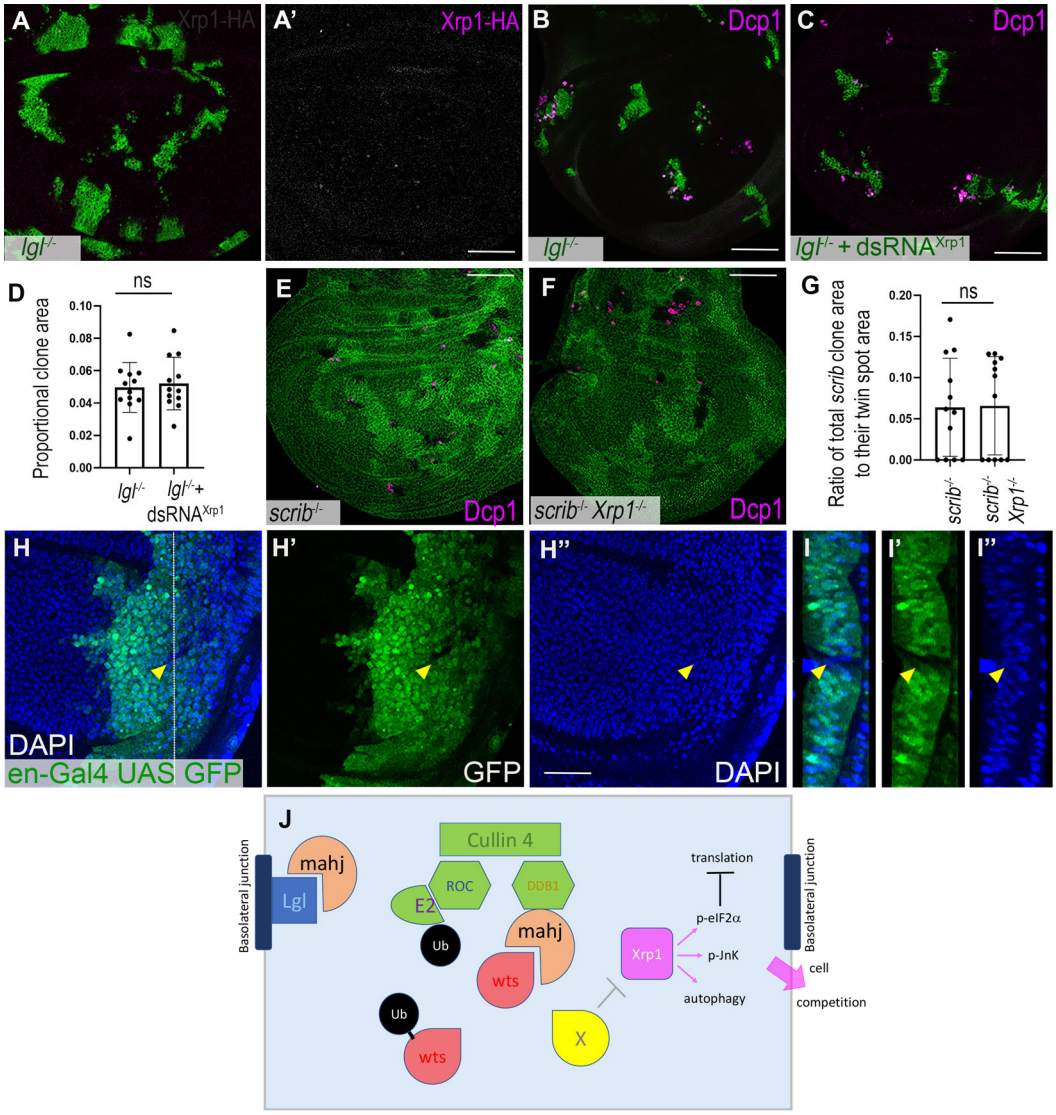

Fig. 7. Polarity defects lead to competition independently of Xrp1. (A-C) Wing discs with *lgl* mutant clones (green). (A,A′) Little Xrp1-HA was induced by *lgl* mutation (magenta; *n*=10). (B) Cell death (magenta) occurred at the boundaries of *lgl* mutant clones. (C,C′) Cell death (magenta) continued at the boundaries of *lgl* mutant clones even after expression of *Xrp1* RNAi (by the tub-Gal4 driver of the FRT40 MARCM stock). (D) Quantification of clone size from genotypes shown in B and C (*n*=12 for both the genotypes). (E) Wing disc with clones of *scrib* mutant cells (black) and reciprocal twin spots (white). Cell death (magenta) occurs near the boundary of *scrib* clones. (F) Wing disc with clones of *scrib* mutant cells depleted for *Xrp1* (black) and reciprocal twin spots (white). Xrp1 depletion did not affect *scrib* mutant cell elimination and competitive cell death (magenta). (G) Quantification of *scrib* mutant clone size with and without *Xrp1* depletion (*n*=12 for both the genotypes). Unpaired *t*-test for quantifications shown in D and G; ns, not significant. Data are mean±s.d. Dots in the graphs represent data from one wing disc. (H) *mahj* knockdown in posterior compartments is associated with patchy loss of the co-expressed GFP marker (arrowhead, observed in 10/17 examples). (H′,H″) The GFP and DAPI channels are also shown separately. Dotted line in H indicates the *x*-axis location reprojected in I-I‴. (I-I‴) Reprojection to show the same preparation from the *y*-axis. Arrowheads indicate that DAPI-labeled nuclei occupy the region lacking GFP label, indicating a loss of GFP expression, not loss of cells. (J) Model for the cellular interactions of Mahj. Mahj interacts physically with Lgl at the basolateral junctions of epithelial cells but does not contribute to the polarity functions of Lgl or to the competitive elimination of *lgl* mutant cells. Instead, *mahj* acts as a substrate receptor protein for Cullin 4 and DDB1, which target Warts and presumably other proteins for ubiquitylation and degradation by the proteosome. One such protein (X in yellow) is a negative regulator of Xrp1. Accordingly, loss of *mahj* function activates Xrp1, a known regulator of eIF2α phosphorylation (and thereby translation), the JNK pathway, autophagy and cell competition. Scale bars: 50 µm.

common spectrum of cellular responses and predispose cells to competitive elimination by wild-type neighbors (Kiparaki et al., 2022). These functional roles for Xrp1 first became apparent through its role in the slow growth, reduced translation and competitive elimination of *Rp*/+ cells, in which *Xrp1* expression is induced in an *rpS12*-dependent manner (Lee et al., 2018; Ji et al., 2019; Kiparaki et al., 2022). In the case of *mahj*, *Xrp1* protein expression is induced to confer a very similar spectrum of cellular effects, but independently of *rpS12* and perhaps depending on stabilization of a protein normally targeted for proteasomal turnover by *mahj*-dependent ubiquitylation. *Xrp1* expression was first found as a *p53*-regulated gene, perhaps part of the DNA damage response (Brodsky et al., 2004; Akdemir et al., 2007). Recently, *Xrp1* induction has also been found as a response to ER stress, possibly through translational regulation downstream of eIF2α phosphorylation (Brown et al., 2021; Ochi et al., 2021; Kiparaki et al., 2022). It has been suggested that eIF2α phosphorylation, and *Xrp1* expression, can also be triggered by a global, cytoplasmic

Development (2022) 149, dev200795. doi:10.1242/dev.200795

proteotoxic stress, which is suggested to occur as a consequence of deficient ribosome assembly in Rp mutant cells (Baumgartner et al., 2021; Langton et al., 2021; Recasens-Alvarez et al., 2021). *Xrp1* expression in response to proteasome inhibition is one piece of evidence for this model (Fig. 4D,D′, Fig. S5B-C′). We show here, however, that *Xrp1* is induced, and cell competition results after loss of *mahj*, a single E3-ligase adapter protein that probably targets only a moderate number of proteins for degradation. Thus, an alternative explanation of *Xrp1* induction after proteasome inhibition is that this could reflect stabilization of one or a few specific proteins. Overall, a picture is emerging of *Xrp1* as a stress-responsive transcription factor whose expression can be initiated by multiple distinct pathways, then leading to a common cellular response, including the elimination of the stressed cells by competition with nearby wild-type cells, when such cells are available (Kiparaki et al., 2022).

Importantly, cells depleted for DCAF1/VprBP, the mammalian homolog of Mahj, are eliminated by competition with wild-type cells in mammalian cell culture (Tamori et al., 2010). Thus, cell competition of *mahj* mutant cells may be a conserved process. Conservation of cell competition has not yet been demonstrated for *Rp*/+ cells in mammals, although it may very well occur (Oliver et al., 2004; Baker, 2020). In mammals, knockdown of either *mahj* or its binding partner *ddb1* results in P53 activation, which is functionally required for the resulting phenotypes (Cang et al., 2006; Han et al., 2020). Differences in *p53* activity lead to cell competition in many mammalian systems (Baker, 2020). *p53* is not required for *mahj*-mediated cell competition in *Drosophila* (Fig. 3A-B′, Fig. S3A-G), but because Xrp1 is a target of *Drosophila p53* in irradiated cells, it is possible *Xrp1* is a p53 target that has replaced the cell competition role of *p53* in *Drosophila*, as has already been suggested for the competition of *Rp*/+ cells, which is also *p53* independent in *Drosophila*, although *Rp* mutations activate *p53* in mammals (Baker et al., 2019). Thus, *mahj*-mediated cell competition may provide another example where Xrp1 mediates a process in *Drosophila* that is dependent on *p53* in mammals.

MATERIALS AND METHODS

Drosophila stocks and genetics

All fly stocks and crosses were maintained at 25°C unless otherwise mentioned. The following fly stocks were used in this study: FRT42 $mahj^{1}$ (Tamori et al., 2010), hsflp UAS GFP; FRT 42 tubgal80; tub Gal4 (a gift from D. J. Pan, UT Southwestern Medical Center, Dallas, TX, USA), hsflp; FRT40tubgal80; tubGal4UAS-GFP (a gift from J. Secombe, Albert Einstein College of Medicine, New York, USA), *Mahj* RNAi (BL:34912), *Xrp1* RNAi [Vienna Drosophila Resource Center (VDRC): 107860], *Xrp1* RNAi (Bloomington Drosophila Stock Center: 34521), $Xrp1^{02515}$ (Spradling et al., 1999), Xrp1-HA (Blanco et al., 2020), En-Gal4-UAS GFP, *White* RNAi (Bloomington Drosophila Stock Center: 33623), $Mahj^{Df}$ (Bloomington Drosophila Stock Center: 5764), 109-68-GAL4 (Bloomington Drosophila Stock Center: 6479), lgl^{4} (Tamori et al., 2010), $Scrib^{1}$ (Bilder et al., 2000), *P53* RNAi (Bloomington Drosophila Stock Center: 41720), *P53*DN (Bloomington Drosophila Stock Center: 8420), *rpr150*-LacZ (Brodsky et al., 2000), $Xrp1^{attp\ FLOX}$ (Blanco et al., 2020), $rps12^{G97D}$ (Kale et al., 2018), *diap*-lacZ (Wu et al., 2008), *ex*-LacZ (Blaumueller and Mlodzik, 2000), *fj*-LacZ (Villano and Katz, 1995), UAS-*hpo* (Udan et al., 2003), UAS-yki, UAS-*ddb1* RNAi (Bloomington Drosophila Stock Center: 41997), *cul4* RNAi (Bloomington Drosophila Stock Center: 50614), UAS-FLAG-$Cul4^{KD}$ (Lin et al., 2009), FRT82B Ubi-mRFP (Bloomington Drosophila Stock Center: 30555), UAS-*ban* (Thompson and Cohen, 2006), FRT82 $Xrp1^{M2\text{-}73}$ (Lee et al., 2018), nub-Gal4 UAS RFP (Bloomington Drosophila Stock Center: 63148), *prosalpha5* RNAi (Bloomington Drosophila Stock Center: 34786), *prosbeta5* (Bloomington Drosophila Stock Center: 34810), *prosbeta6* (Bloomington Drosophila Stock Center: 34801), UAS-*PPP1R15* (Bloomington Drosophila Stock Center: 76250), Wts RNAi (VDRC: 106174), UAS-Wts-myc (Ch-II, a gift from Kenneth Irvine's lab, Waksman Institute, Piscataway, NJ, USA), Roc1a RNAi (VDRC: 32399) and P{GAL4-Act5C(FRT-CD2).P}S (Bloomington Drosophila Stock Center: 51308).

Mosaic analysis

Loss- or gain-of-function somatic clones were generated using FLP/FRT-mediated mitotic recombination. To induce somatic loss- or gain-of-function clones using heat shock flippase (hsflp), heat shock was given for either 15 min or 30 min for *cis* or *trans*-chromosomal recombination, respectively, at 60±12 h after egg laying, and dissection was carried out 72±12 h after heat shock. To control hs-FLP copy number in different genotypes, only male larvae were selected for experiments where clone areas in wing discs of different genotypes were compared.

Immunohistochemistry and imaging

Wandering third instar were dissected in 1×PBS buffer and fixation was carried out in 4% paraformaldehyde (in 1×PBS buffer). Fixed imaginal discs were washed in PBT (0.3% Triton X-100, 1×PBS) three times for 10 min each. Incubation of imaginal discs with primary antibody was carried out overnight at 4°C. After overnight incubation, washing was carried out thrice with PBT for 10 min each. Secondary antibody incubation was carried out at room temperature followed by three washes with PBT for 10 min each. Primary antibodies used in this study were mouse anti-βGal (1:100, Developmental Studies Hybridoma Bank, mAb40-1a) (Ghattas et al., 1991), rabbit anti-active-Dcp1 (1:100, Cell Signaling technology, 9578), mouse anti-HA (1:100, Cell Signaling Technology, 2367) and rabbit pJNK (1:200, Promega, V793B). Secondary antibodies used were Cy2 and Cy5 conjugates (1:200, Jackson ImmunoResearch, 115-225-166 and 711-175-152, respectively), and goat anti-mouse and anti-rabbit Alexa Fluor 555 (1:400, Thermo Fisher Scientific, A11001 and A21429, respectively). To measure global translation, a Click-iT Plus OPP Alexa Fluor 594 Protein Synthesis Assay Kit (Thermo Fisher Scientific, C10457) was used as described previously (Lee et al., 2018). For lysosomal activity detection, Lysotracker red DND-99 (Thermo Fisher Scientific) was used at the concentration of 4 µM and staining was carried out in Schneider's *Drosophila* Medium with 10% FBS for 40 min. To measure cell death after irradiation, larvae within food vials were exposed to 4000 rad γ-rays at 72±12 h after egg laying while dissection was carried out 72 h post irradiation. Images were acquired using SP8 confocal microscopes (Leica) followed by processing of images with NIH ImageJ and Adobe Photoshop software. ImageJ was used to measure clone area and clone perimeter, and to quantify fluorescence signal intensity of a wing disc. To make *z* projections for the wing disc with mutant or control clones, equal numbers of sections were combined while avoiding basal sections. Dying cells marked by anti-Dcp1 on the clone perimeter were counted as competitive cell death. To calculate dying cells per unit of clone perimeter, the total number of dying cells at the clone boundary were divided by the length of the clone perimeter of a wing disc. Analysis was not carried out blind. All samples acquired were analyzed and no method of randomization used. Number of wing discs analyzed are reported as *n* values in figure legends. Sample sizes were based on previous experience with similar experiments and not determined by statistical methods. All experiments assessing cell competition and all but one experiment overall were independently performed on at least two occasions. The exception was p53 RNAi after irradiation (Fig. S3C). Data presented graphically represent mean values, e.g. mean clone area or mean cell death. Error bars represent ±1 s.d. Statistical comparisons were generally made using *t*-test assuming normal distribution. When $n<10$, or for ratios between clone and twin-spot sizes, the Mann–Whitney test was used. The Wilcoxon matched-pairs test was used to compare fluorescence signal of anterior and posterior signal (Fig. S4G). No adjustments were made for multiple comparisons. *P*-values are provided in the figure legends.

Acknowledgements

We thank Drs W.-M. Deng, C.-T. Chien, K. Irvine, D. Pan, J. Secombe and H. Wang for fly stocks. Other fly stocks were obtained from the Bloomington Drosophila Stock Center (supported by NIH P40OD018537) and the Vienna Drosophila Resource

Center. We thank Drs A. Jenny, C. Khan, M. Kiparaki and S. Nair for comments on manuscript, Dr Kiparaki for sharing unpublished data, and Dr Khan for sharing unpublished fly stocks. Confocal microscopy was performed in the Analytical Imaging Facility of the Albert Einstein College of Medicine (supported by the NCI P30CA013330) using the Leica SP8 microscope acquired through NIH SIG 1S10 OD023591. The monoclonal antibody mAb40-1a developed by J. R. Sanes was obtained from the Developmental Studies Hybridoma Bank, created by the NICHD and maintained at the University of Iowa, Department of Biology, Iowa City, IA 52242.

Competing interests
The authors declare no competing or financial interests.

Author contributions
Conceptualization: A.K., N.E.B.; Methodology: A.K.; Validation: A.K.; Formal analysis: A.K.; Investigation: A.K.; Data curation: A.K.; Writing - original draft: A.K.; Writing - review & editing: N.E.B.; Visualization: A.K.; Supervision: N.E.B.; Funding acquisition: N.E.B.

Funding
This project was supported by the National Institutes of Health (GM104213). Deposited in PMC for release after 12 months.

Peer review history
The peer review history is available online at https://journals.biologists.com/dev/lookup/doi/10.1242/dev.200795.reviewer-comments.pdf.

References
Akdemir, F., Christich, A., Sogame, N., Chapo, J. and Abrams, J. M. (2007). p53 directs focused genomic responses in Drosophila. *Oncogene* **26**, 5184-5193. doi:10.1038/sj.onc.1210328

Angers, S., Li, T., Yi, X., Maccoss, M. J., Moon, R. T. and Zheng, N. (2006). Molecular architecture and assembly of the DDB1-CUL4A ubiquitin ligase machinery. *Nature* **443**, 590-593. doi:10.1038/nature05175

Baillon, L., Germani, F., Rockel, C., Hilchenbach, J. and Basler, K. (2018). Xrp1 is a transcription factor required for cell competition-driven elimination of loser cells. *Sci. Rep.* **8**, 17712. doi:10.1038/s41598-018-36277-4

Baker, N. E. (2011). Cell competition. *Curr. Biol.* **21**, R11-R15. doi:10.1016/j.cub.2010.11.030

Baker, N. E. (2020). Emerging mechanisms of cell competition. *Nat. Rev. Genet.* **21**, 683-697. doi:10.1038/s41576-020-0262-8

Baker, N. E., Kiparaki, M. and Khan, C. (2019). A potential link between p53, cell competition and ribosomopathy in mammals and in Drosophila. *Dev. Biol.* **446**, 17-19. doi:10.1016/j.ydbio.2018.11.018

Baumgartner, M. E., Dinan, M. P., Langton, P. F., Kucinski, I. and Piddini, E. (2021). Proteotoxic stress is a driver of the loser status and cell competition. *Nat. Cell Biol.* **23**, 136-146. doi:10.1038/s41556-020-00627-0

Ben-David, U. and Amon, A. (2020). Context is everything: aneuploidy in cancer. *Nat. Rev. Genet.* **21**, 44-62. doi:10.1038/s41576-019-0171-x

Bilder, D. and Perrimon, N. (2000). Localization of apical epithelial determinants by the basolateral PDZ protein Scribble. *Nature* **403**, 676-680. doi:10.1038/35001108

Bilder, D., Li, M. and Perrimon, N. (2000). Cooperative regulation of cell polarity and growth by Drosophila tumor suppressors. *Science* **289**, 113-116. doi:10.1126/science.289.5476.113

Blanco, J., Cooper, J. C. and Baker, N. E. (2020). Roles of C/EBP class bZip proteins in the growth and cell competition of Rp ('Minute') mutants in Drosophila. *Elife* **9**, e50535. doi:10.7554/eLife.50535

Blaumueller, C. M. and Mlodzik, M. (2000). The Drosophila tumor suppressor expanded regulates growth, apoptosis, and patterning during development. *Mech. Dev.* **92**, 251-262. doi:10.1016/S0925-4773(00)00246-X

Bridges, C. B. and Morgan, T. H. (1923). The third-chromosome group of mutant characters of Drosophila melanogaster. *Publs. Carnegie Instn.* **327**, 1-251.

Brodsky, M. H., Nordstrom, W., Tsang, G., Kwan, E., Rubin, G. M. and Abrams, J. M. (2000). Drosophila p53 binds a damage response element at the reaper locus. *Cell* **101**, 103-113. doi:10.1016/S0092-8674(00)80627-3

Brodsky, M. H., Weinert, B. T., Tsang, G., Rong, Y. S., Mcginnis, N. M., Golic, K. G., Rio, D. C. and Rubin, G. M. (2004). Drosophila melanogaster MNK/Chk2 and p53 regulate multiple DNA repair and apoptotic pathways following DNA damage. *Mol. Cell. Biol.* **24**, 1219-1231. doi:10.1128/MCB.24.3.1219-1231.2004

Brown, B., Mitra, S., Roach, F. D., Vasudevan, D. and Ryoo, H. D. (2021). The transcription factor Xrp1 is required for PERK-mediated antioxidant gene induction in Drosophila. *Elife* **10**, e74047. doi:10.7554/eLife.74047

Cang, Y., Zhang, J., Nicholas, S. A., Bastien, J., Li, B., Zhou, P. and Goff, S. P. (2006). Deletion of DDB1 in mouse brain and lens leads to p53-dependent elimination of proliferating cells. *Cell* **127**, 929-940. doi:10.1016/j.cell.2006.09.045

Chen, C. L., Schroeder, M. C., Kango-Singh, M., Tao, C. and Halder, G. (2012). Tumor suppression by cell competition through regulation of the Hippo pathway. *Proc. Natl. Acad. Sci. USA* **109**, 484-489. doi:10.1073/pnas.1113882109

Cho, E., Feng, Y., Rauskolb, C., Maitra, S., Fehon, R. and Irvine, K. D. (2006). Delineation of a Fat tumor suppressor pathway. *Nat. Genet.* **38**, 1142-1150. doi:10.1038/ng1887

Clavería, C. and Torres, M. (2016). Cell competition: mechanisms and physiological roles. *Annu. Rev. Cell Dev. Biol.* **32**, 411-439. doi:10.1146/annurev-cellbio-111315-125142

Cooper, J. and Giancotti, F. G. (2014). Molecular insights into NF2/Merlin tumor suppressor function. *FEBS Lett.* **588**, 2743-2752. doi:10.1016/j.febslet.2014.04.001

Dang, C. V. (2012). MYC on the path to cancer. *Cell* **149**, 22-35. doi:10.1016/j.cell.2012.03.003

De La Cova, C., Abril, M., Bellosta, P., Gallant, P. and Johnston, L. A. (2004). Drosophila myc regulates organ size by inducing cell competition. *Cell* **117**, 107-116. doi:10.1016/S0092-8674(04)00214-4

Dekanty, A., Barrio, L., Muzzopappa, M., Auer, H. and Milán, M. (2012). Aneuploidy-induced delaminating cells drive tumorigenesis in Drosophila epithelia. *Proc. Natl. Acad. Sci. USA* **109**, 20549-20554. doi:10.1073/pnas.1206675109

Di Giacomo, S., Sollazzo, M., De Biase, D., Ragazzi, M., Bellosta, P., Pession, A. and Grifoni, D. (2017). Human cancer cells signal their competitive fitness through MYC activity. *Sci. Rep.* **7**, 12568. doi:10.1038/s41598-017-13002-1

Dong, J., Feldmann, G., Huang, J., Wu, S., Zhang, N., Comerford, S. A., Gayyed, M. F., Anders, R. A., Maitra, A. and Pan, D. (2007). Elucidation of a universal size-control mechanism in Drosophila and mammals. *Cell* **130**, 1120-1133. doi:10.1016/j.cell.2007.07.019

Froldi, F., Ziosi, M., Garoia, F., Pession, A., Grzeschik, N. A., Bellosta, P., Strand, D., Richardson, H. E., Pession, A. and Grifoni, D. (2010). The lethal giant larvae tumour suppressor mutation requires dMyc oncoprotein to promote clonal malignancy. *BMC Biol.* **8**, 33. doi:10.1186/1741-7007-8-33

Ghattas, I. R., Sanes, J. R. and Majors, J. E. (1991). The encephalomyocarditis virus internal ribosome entry site allows efficient coexpression of two genes from a recombinant provirus in cultured cells and in embryos. *Mol. Cell. Biol.* **11**, 5848-5859. doi:10.1128/mcb.11.12.5848-5859.1991

Guo, Z., Kong, Q., Liu, C., Zhang, S., Zou, L., Yan, F., Whitmire, J. K., Xiong, Y., Chen, X. and Wan, Y. Y. (2016). DCAF1 controls T-cell function via p53-dependent and -independent mechanisms. *Nat. Commun.* **7**, 10307. doi:10.1038/ncomms10307

Hamaratoglu, F., Willecke, M., Kango-Singh, M., Nolo, R., Hyun, E., Tao, C., Jafar-Nejad, H. and Halder, G. (2006). The tumour-suppressor genes NF2/Merlin and Expanded act through Hippo signalling to regulate cell proliferation and apoptosis. *Nat. Cell Biol.* **8**, 27-36. doi:10.1038/ncb1339

Han, X. R., Sasaki, N., Jackson, S. C., Wang, P., Li, Z., Smith, M. D., Xie, L., Chen, X., Zhang, Y., Marzluff, W. F. et al. (2020). CRL4(DCAF1/VprBP) E3 ubiquitin ligase controls ribosome biogenesis, cell proliferation, and development. *Sci. Adv.* **6**, eabd6078. doi:10.1126/sciadv.abd6078

Hao, Y., Chun, A., Cheung, K., Rashidi, B. and Yang, X. (2008). Tumor suppressor LATS1 is a negative regulator of oncogene YAP. *J. Biol. Chem.* **283**, 5496-5509. doi:10.1074/jbc.M709037200

He, Y. J., Mccall, C. M., Hu, J., Zeng, Y. and Xiong, Y. (2006). DDB1 functions as a linker to recruit receptor WD40 proteins to CUL4-ROC1 ubiquitin ligases. *Genes Dev.* **20**, 2949-2954. doi:10.1101/gad.1483206

Hershko, A. and Ciechanover, A. (1998). The ubiquitin system. *Annu. Rev. Biochem.* **67**, 425-479. doi:10.1146/annurev.biochem.67.1.425

Hrecka, K., Gierszewska, M., Srivastava, S., Kozaczkiewicz, L., Swanson, S. K., Florens, L., Washburn, M. P. and Skowronski, J. (2007). Lentiviral Vpr usurps Cul4-DDB1[VprBP] E3 ubiquitin ligase to modulate cell cycle. *Proc. Natl. Acad. Sci. USA* **104**, 11778-11783. doi:10.1073/pnas.0702102104

Huang, J., Wu, S., Barrera, J., Matthews, K. and Pan, D. (2005). The Hippo signaling pathway coordinately regulates cell proliferation and apoptosis by inactivating Yorkie, the Drosophila Homolog of YAP. *Cell* **122**, 421-434. doi:10.1016/j.cell.2005.06.007

Humbert, P., Russell, S. and Richardson, H. (2003). Dlg, scribble and Lgl in cell polarity, cell proliferation and cancer. *BioEssays* **25**, 542-553. doi:10.1002/bies.10286

Igaki, T., Pagliarini, R. A. and Xu, T. (2006). Loss of cell polarity drives tumor growth and invasion through JNK activation in Drosophila. *Curr. Biol.* **16**, 1139-1146. doi:10.1016/j.cub.2006.04.042

Ji, Z., Kiparaki, M., Folgado, V., Kumar, A., Blanco, J., Rimesso, G., Chuen, J., Liu, Y., Zheng, D. and Baker, N. E. (2019). Drosophila RpS12 controls translation, growth, and cell competition through Xrp1. *PLoS Genet.* **15**, e1008513. doi:10.1371/journal.pgen.1008513

Ji, Z., Chuen, J., Kiparaki, M. and Baker, N. (2021). Cell competition removes segmental aneuploid cells from Drosophila imaginal disc-derived tissues based on ribosomal protein gene dose. *Elife* **10**, e61172. doi:10.7554/eLife.61172

Justice, R. W., Zilian, O., Woods, D. F., Noll, M. and Bryant, P. J. (1995). The Drosophila tumor suppressor gene warts encodes a homolog of human myotonic

dystrophy kinase and is required for the control of cell shape and proliferation. *Genes Dev.* **9**, 534-546. doi:10.1101/gad.9.5.534

Kale, A., Li, W., Lee, C. H. and Baker, N. E. (2015). Apoptotic mechanisms during competition of ribosomal protein mutant cells: roles of the initiator caspases Dronc and Dream/Strica. *Cell Death Differ.* **22**, 1300-1312. doi:10.1038/cdd.2014.218

Kale, A., Ji, Z., Kiparaki, M., Blanco, J., Rimesso, G., Flibotte, S. and Baker, N. E. (2018). Ribosomal protein S12e has a distinct function in cell competition. *Dev. Cell* **44**, 42-55.e4. doi:10.1016/j.devcel.2017.12.007

Khan, S. J., Bajpai, A., Alam, M. A., Gupta, R. P., Harsh, S., Pandey, R. K., Goel-Bhattacharya, S., Nigam, A., Mishra, A. and Sinha, P. (2013). Epithelial neoplasia in Drosophila entails switch to primitive cell states. *Proc. Natl. Acad. Sci. USA* **110**, E2163-E2172. doi:10.1073/pnas.1206392110

Kiparaki, M., Khan, C., Folgado-Marco, V., Chuen, J., Moulos, P. and Baker, N. E. (2022). The transcription factor Xrp1 orchestrates both reduced translation and cell competition upon defective ribosome assembly or function. *Elife* **11**, e71705. doi:10.7554/eLife.71705

Kucinski, I., Dinan, M., Kolahgar, G. and Piddini, E. (2017). Chronic activation of JNK JAK/STAT and oxidative stress signalling causes the loser cell status. *Nat. Commun.* **8**, 136. doi:10.1038/s41467-017-00145-y

Lai, Z. C., Wei, X., Shimizu, T., Ramos, E., Rohrbaugh, M., Nikolaidis, N., Ho, L. L. and Li, Y. (2005). Control of cell proliferation and apoptosis by mob as tumor suppressor, mats. *Cell* **120**, 675-685. doi:10.1016/j.cell.2004.12.036

Lambertsson, A. (1998). The *Minute* genes in *Drosophila* and their molecular functions. *Adv. Genet.* **38**, 69-134. doi:10.1016/S0065-2660(08)60142-X

Langton, P. F., Baumgartner, M. E., Logeay, R. and Piddini, E. (2021). Xrp1 and Irbp18 trigger a feed-forward loop of proteotoxic stress to induce the loser status. *PLoS Genet.* **17**, e1009946. doi:10.1371/journal.pgen.1009946

Le Rouzic, E., Belaidouni, N., Estrabaud, E., Morel, M., Rain, J. C., Transy, C. and Margottin-Goguet, F. (2007). HIV1 Vpr arrests the cell cycle by recruiting DCAF1/VprBP, a receptor of the Cul4-DDB1 ubiquitin ligase. *Cell Cycle* **6**, 182-188. doi:10.4161/cc.6.2.3732

Lee, C.-H., Rimesso, G., Reynolds, D. M., Cai, J. and Baker, N. E. (2016). Whole-genome sequencing and iPLEX MassARRAY genotyping map an EMS-induced mutation affecting cell competition in Drosophila melanogaster. *G3* **6**, 3207-3217. doi:10.1534/g3.116.029421

Lee, C.-H., Kiparaki, M., Blanco, J., Folgado, V., Ji, Z., Kumar, A., Rimesso, G. and Baker, N. E. (2018). A regulatory response to ribosomal protein mutations controls translation, growth, and cell competition. *Dev. Cell* **46**, 807. doi:10.1016/j.devcel.2018.09.009

Levayer, R. and Moreno, E. (2013). Mechanisms of cell competition: themes and variations. *J. Cell Biol.* **200**, 689-698. doi:10.1083/jcb.201301051

Li, W. and Baker, N. E. (2007). Engulfment is required for cell competition. *Cell* **129**, 1215-1225. doi:10.1016/j.cell.2007.03.054

Li, R. and Zhu, J. (2022). Effects of aneuploidy on cell behaviour and function. *Nat. Rev. Mol. Cell Biol.* **23**, 250-265. doi:10.1038/s41580-021-00436-9

Li, W., Cooper, J., Zhou, L., Yang, C., Erdjument-Bromage, H., Zagzag, D., Snuderl, M., Ladanyi, M., Hanemann, C. O., Zhou, P. et al. (2014). Merlin/NF2 loss-driven tumorigenesis linked to CRL4(DCAF1)-mediated inhibition of the hippo pathway kinases Lats1 and 2 in the nucleus. *Cancer Cell* **26**, 48-60. doi:10.1016/j.ccr.2014.05.001

Lin, H. C., Wu, J. T., Tan, B. C. and Chien, C. T. (2009). Cul4 and DDB1 regulate Orc2 localization, BrdU incorporation and Dup stability during gene amplification in Drosophila follicle cells. *J. Cell Sci.* **122**, 2393-2401. doi:10.1242/jcs.042861

Liu, Z., Yee, P. P., Wei, Y., Liu, Z., Kawasawa, Y. I. and Li, W. (2019). Differential YAP expression in glioma cells induces cell competition and promotes tumorigenesis. *J. Cell Sci.* **132**, jcs225714. doi:10.1242/jcs.225714

Lubow, J. and Collins, K. L. (2020). Vpr is a VIP: HIV Vpr and infected macrophages promote viral pathogenesis. *Viruses* **12**, 809. doi:10.3390/v12080809

Ly, P. T., Tan, Y. S., Koe, C. T., Zhang, Y., Xie, G., Endow, S., Deng, W. M., Yu, F. and Wang, H. (2019). CRL4Mahj E3 ubiquitin ligase promotes neural stem cell reactivation. *PLoS Biol.* **17**, e3000276. doi:10.1371/journal.pbio.3000276

Madan, E., Pelham, C. J., Nagane, M., Parker, T. M., Canas-Marques, R., Fazio, K., Shaik, K., Yuan, Y., Henriques, V., Galzerano, A. et al. (2019). Flower isoforms promote competitive growth in cancer. *Nature* **572**, 260-264. doi:10.1038/s41586-019-1429-3

Marygold, S. J., Roote, J., Reuter, G., Lambertsson, A., Ashburner, M., Millburn, G. H., Harrison, P. M., Yu, Z., Kenmochi, N., Kaufman, T. C. et al. (2007). The ribosomal protein genes and Minute loci of Drosophila melanogaster. *Genome Biol.* **8**, R216. doi:10.1186/gb-2007-8-10-r216

Mccall, C. M., Miliani De Marval, P. L., Chastain, P. D., 2ND, Jackson, S. C., He, Y. J., Kotake, Y., Cook, J. G. and Xiong, Y. (2008). Human immunodeficiency virus type 1 Vpr-binding protein VprBP, a WD40 protein associated with the DDB1-CUL4 E3 ubiquitin ligase, is essential for DNA replication and embryonic development. *Mol. Cell. Biol.* **28**, 5621-5633. doi:10.1128/MCB.00232-08

Menendez, J., Perez-Garijo, A., Calleja, M. and Morata, G. (2010). A tumor-suppressing mechanism in Drosophila involving cell competition and the Hippo pathway. *Proc. Natl. Acad. Sci. USA* **107**, 14651-14656. doi:10.1073/pnas.1009376107

Molina, O., Abad, M. A., Sole, F. and Menendez, P. (2021). Aneuploidy in cancer: lessons from acute lymphoblastic leukemia. *Trends Cancer* **7**, 37-47. doi:10.1016/j.trecan.2020.08.008

Morata, G. (2021). Cell competition: a historical perspective. *Dev. Biol.* **476**, 33-40. doi:10.1016/j.ydbio.2021.02.012

Morata, G. and Ripoll, P. (1975). Minutes: mutants of drosophila autonomously affecting cell division rate. *Dev. Biol.* **42**, 211-221. doi:10.1016/0012-1606(75)90330-9

Moreno, E. and Basler, K. (2004). dMyc transforms cells into super-competitors. *Cell* **117**, 117-129. doi:10.1016/S0092-8674(04)00262-4

Moreno, E., Basler, K. and Morata, G. (2002). Cells compete for decapentaplegic survival factor to prevent apoptosis in Drosophila wing development. *Nature* **416**, 755-759. doi:10.1038/416755a

Moroishi, T., Hansen, C. G. and Guan, K. L. (2015). The emerging roles of YAP and TAZ in cancer. *Nat. Rev. Cancer* **15**, 73-79. doi:10.1038/nrc3876

Moya, I. M., Castaldo, S. A., Van Den Mooter, L., Soheily, S., Sansores-Garcia, L., Jacobs, J., Mannaerts, I., Xie, J., Verboven, E., Hillen, H. et al. (2019). Peritumoral activation of the Hippo pathway effectors YAP and TAZ suppresses liver cancer in mice. *Science* **366**, 1029-1034. doi:10.1126/science.aaw9886

Nagata, R. and Igaki, T. (2018). Cell competition: Emerging mechanisms to eliminate neighbors. *Dev. Growth Differ.* **60**, 522-530. doi:10.1111/dgd.12575

Nagata, R., Nakamura, M., Sanaki, Y. and Igaki, T. (2019). Cell competition is driven by autophagy. *Dev. Cell* **51**, 99-112 e4. doi:10.1016/j.devcel.2019.08.018

Nagata, R., Akai, N., Kondo, S., Saito, K., Ohsawa, S. and Igaki, T. (2022). Yorkie drives supercompetition by non-autonomous induction of autophagy via bantam microRNA in Drosophila. *Curr. Biol.* **32**, 1064-1076.e4. doi:10.1016/j.cub.2022.01.016

Neto-Silva, R. M., De Beco, S. and Johnston, L. A. (2010). Evidence for a growth-stabilizing regulatory feedback mechanism between Myc and Yorkie, the Drosophila homolog of Yap. *Dev. Cell* **19**, 507-520. doi:10.1016/j.devcel.2010.09.009

Ochi, N., Nakamura, M., Nagata, R., Wakasa, N., Nakano, R. and Igaki, T. (2021). Cell competition is driven by Xrp1-mediated phosphorylation of eukaryotic initiation factor 2α. *PLoS Genet.* **17**, e1009958. doi:10.1371/journal.pgen.1009958

Oliver, E. R., Saunders, T. L., Tarlé, S. A. and Glaser, T. (2004). Ribosomal protein L24 defect in belly spot and tail (*Bst*), a mouse Minute. *Development* **131**, 3907-3920. doi:10.1242/dev.01268

Pan, Z. Q., Kentsis, A., Dias, D. C., Yamoah, K. and Wu, K. (2004). Nedd8 on cullin: building an expressway to protein destruction. *Oncogene* **23**, 1985-1997. doi:10.1038/sj.onc.1207414

Pantalacci, S., Tapon, N. and Léopold, P. (2003). The Salvador partner Hippo promotes apoptosis and cell-cycle exit in Drosophila. *Nat. Cell Biol.* **5**, 921-927. doi:10.1038/ncb1051

Parker, T. M., Gupta, K., Palma, A. M., Yekelchyk, M., Fisher, P. B., Grossman, S. R., Won, K. J., Madan, E., Moreno, E. and Gogna, R. (2021). Cell competition in intratumoral and tumor microenvironment interactions. *EMBO J.* **40**, e107271. doi:10.15252/embj.2020107271

Patel, M. S., Shah, H. S. and Shrivastava, N. (2017). c-Myc-dependent cell competition in human cancer cells. *J. Cell. Biochem.* **118**, 1782-1791. doi:10.1002/jcb.25846

Petroski, M. D. and Deshaies, R. J. (2005). Function and regulation of cullin-RING ubiquitin ligases. *Nat. Rev. Mol. Cell Biol.* **6**, 9-20. doi:10.1038/nrm1547

Recasens-Alvarez, C., Alexandre, C., Kirkpatrick, J., Nojima, H., Huels, D. J., Snijders, A. P. and Vincent, J. P. (2021). Ribosomopathy-associated mutations cause proteotoxic stress that is alleviated by TOR inhibition. *Nat. Cell Biol.* **23**, 127-135. doi:10.1038/s41556-020-00626-1

Ryoo, H. D. and Vasudevan, D. (2017). Two distinct nodes of translational inhibition in the Integrated Stress Response. *BMB Rep.* **50**, 539-545. doi:10.5483/BMBRep.2017.50.11.157

Sang, Y., Yan, F. and Ren, X. (2015). The role and mechanism of CRL4 E3 ubiquitin ligase in cancer and its potential therapy implications. *Oncotarget* **6**, 42590-42602. doi:10.18632/oncotarget.6052

Simpson, P. and Morata, G. (1981). Differential mitotic rates and patterns of growth in compartments in the Drosophila wing. *Dev. Biol.* **85**, 299-308. doi:10.1016/0012-1606(81)90261-X

Spradling, A. C., Stern, D. F., Beaton, A., Rhem, E. J., Laverty, T., Mozden, N., Misra, S. and Rubin, G. M. (1999). The BDGP gene disruption project: single P-element insertions mutating 25% of vital *Drosophila* genes. *Genetics* **153**, 135-177. doi:10.1093/genetics/153.1.135

Suijkerbuijk, S. J., Kolahgar, G., Kucinski, I. and Piddini, E. (2016). Cell competition drives the growth of intestinal adenomas in Drosophila. *Curr. Biol.* **26**, 428-438. doi:10.1016/j.cub.2015.12.043

Tamori, Y., Bialucha, C. U., Tian, A.-G., Kajita, M., Huang, Y.-C., Norman, M., Harrison, N., Poulton, J., Ivanovitch, K., Disch, L. et al. (2010). Involvement of Lgl and Mahjong/VprBP in cell competition. *PLoS Biol.* **8**, e1000422. doi:10.1371/journal.pbio.1000422

Tan, L., Ehrlich, E. and Yu, X. F. (2007). DDB1 and Cul4A are required for human immunodeficiency virus type 1 Vpr-induced G2 arrest. *J. Virol.* **81**, 10822-10830. doi:10.1128/JVI.01380-07

Tare, M., Sarkar, A., Bedi, S., Kango-Singh, M. and Singh, A. (2016). Cullin-4 regulates Wingless and JNK signaling-mediated cell death in the Drosophila eye. *Cell Death Dis.* **7**, e2566. doi:10.1038/cddis.2016.338

Thompson, B. J. and Cohen, S. M. (2006). The Hippo pathway regulates the bantam microRNA to control cell proliferation and apoptosis in Drosophila. *Cell* **126**, 767-774. doi:10.1016/j.cell.2006.07.013

Tyler, D. M. and Baker, N. E. (2007). Expanded and fat regulate growth and differentiation in the Drosophila eye through multiple signaling pathways. *Dev. Biol.* **305**, 187-201. doi:10.1016/j.ydbio.2007.02.004

Tyler, D. M., Li, W., Zhuo, N., Pellock, B. and Baker, N. E. (2007). Genes affecting cell competition in Drosophila. *Genetics* **175**, 643-657. doi:10.1534/genetics.106.061929

Udan, R. S., Kango-Singh, M., Nolo, R., Tao, C. and Halder, G. (2003). Hippo promotes proliferation arrest and apoptosis in the Salvador/Warts pathway. *Nat. Cell Biol.* **5**, 914-920. doi:10.1038/ncb1050

Uechi, T., Tanaka, T. and Kenmochi, N. (2001). A complete map of the human ribosomal protein genes: assignment of 80 genes to the cytogenetic map and implications for human disorders. *Genomics* **72**, 223-230. doi:10.1006/geno.2000.6470

Vaughen, J. and Igaki, T. (2016). Slit-Robo repulsive signaling extrudes tumorigenic cells from Epithelia. *Dev. Cell* **39**, 683-695. doi:10.1016/j.devcel.2016.11.015

Villano, J. L. and Katz, F. N. (1995). four-jointed is required for intermediate growth in the proximal-distal axis in Drosophila. *Development* **121**, 2767-2777. doi:10.1242/dev.121.9.2767

Wang, L. H. and Baker, N. E. (2015). Salvador-Warts-Hippo pathway in a developmental checkpoint monitoring helix-loop-helix proteins. *Dev. Cell* **32**, 191-202. doi:10.1016/j.devcel.2014.12.002

Wek, R. C. (2018). Role of eIF2α kinases in translational control and adaptation to cellular stress. *Cold Spring Harb. Perspect. Biol.* **10**, a032870. doi:10.1101/cshperspect.a032870

Wu, S., Huang, J., Dong, J. and Pan, D. (2003). hippo encodes a Ste-20 family protein kinase that restricts cell proliferation and promotes apoptosis in conjunction with salvador and warts. *Cell* **114**, 445-456. doi:10.1016/S0092-8674(03)00549-X

Wu, S., Liu, Y., Zheng, Y., Dong, J. and Pan, D. (2008). The TEAD/TEF family protein Scalloped mediates transcriptional output of the Hippo growth-regulatory pathway. *Dev. Cell* **14**, 388-398. doi:10.1016/j.devcel.2008.01.007

Yamamoto, M., Ohsawa, S., Kunimasa, K. and Igaki, T. (2017). The ligand Sas and its receptor PTP10D drive tumour-suppressive cell competition. *Nature* **542**, 246-250. doi:10.1038/nature21033

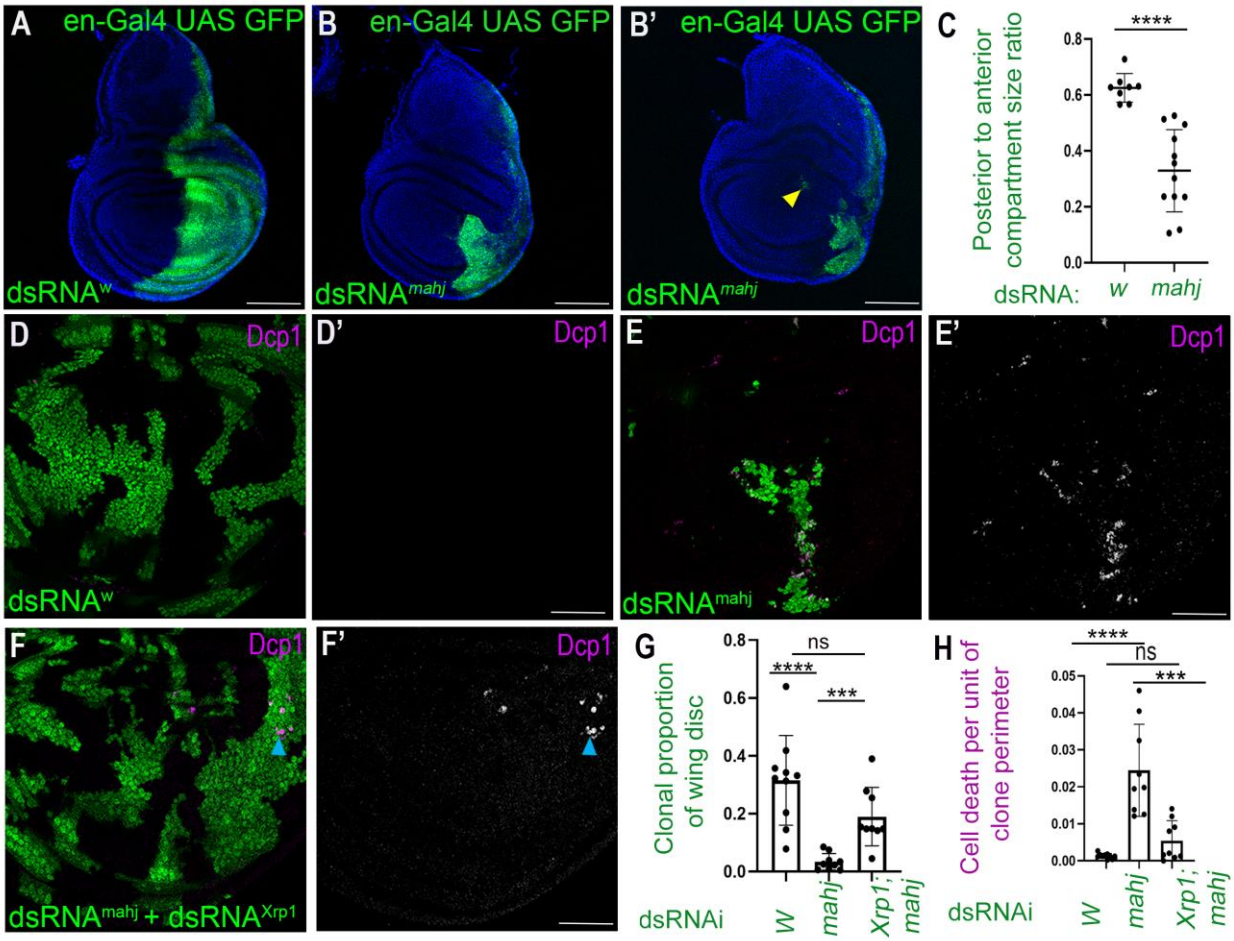

Fig. S1. Cell competition and growth perturbation after *mahj* knockdown

(A-B') Wing disc expressing *white* (A) or *mahj* RNAi (B, B') in the posterior compartment (green, engrailed driver). Knockdown of *mahj* in posterior compartment results in mild (B) to severe (B') size reduction. (Note loss of compartment shape and GFP positive cells in the anterior compartment (yellow arrowhead, (B')) upon *mahj* knockdown in the posterior compartment. N =8 and 12 for panel A and B, respectively. (C) Quantification of compartment size. (D-F) Wing discs with mosaic clones (green) expressing RNAi for *white* (D-D'), *mahj* (E-E'), *Xrp1*, *mahj* (F-F') under flipout act-gal4 driver and stained for Anti-Dcp1 to mark dying cells (magenta). N= 9, 12 & 12 for panel D, E & F, respectively. (E-E') *mahj* knockdown resulted in smaller clones with Dcp1 marked cells at clone boundaries . (F-F') However, simultaneous knockdown of *Xrp1* along with *mahj* rescued

clone size and boundary cell death . Occasional cell death was observed in clones (cyan arrowhead). (G) Quantification of clone size upon knockdown of *white*, *mahj* and *mahj* & *Xrp1*. (H) Cell death quantification at the clone boundary in the three genotypes presented in (D-F'). Dots in the graph C, G and H represent data from single wing disc, statistical test used: Mann-Whitney test, **** P<0.0001, *** P≤ 0.0003, ns = not significant, SD = error bars, scale bar: 50 μm.

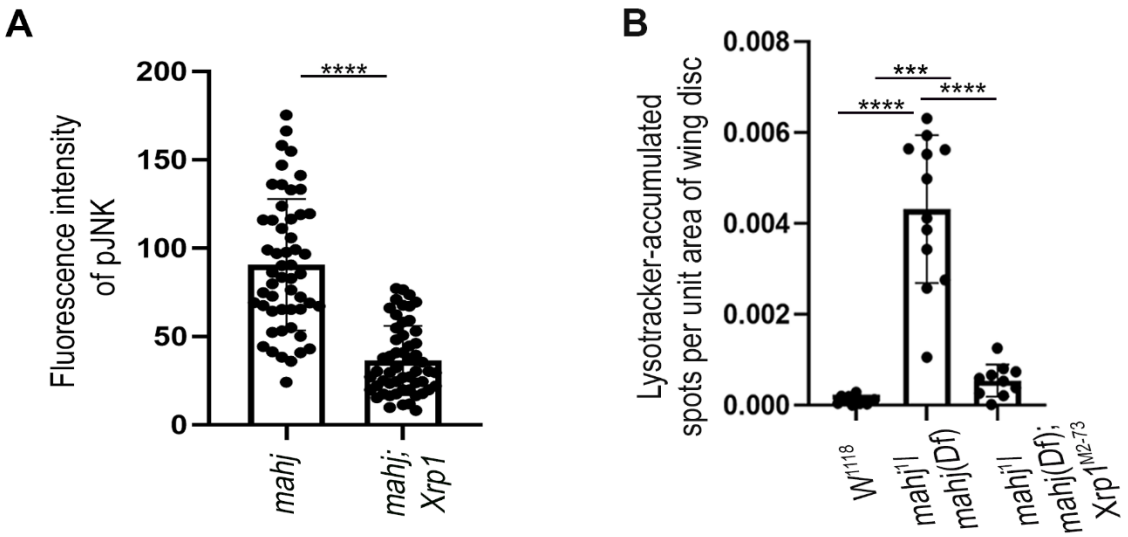

Fig. S2. Quantification of Fig 2A-B, C-E

(A) Quantification of p-JNK levels in *mahj* mutant clones and one with knockdown of Xrp1. Dots in the graph represent signal intensity of p-JNK in the individual mutant clones of a wing disc. (B) Quantification of lysotracker dye punta in wild type, *mahj* and *mahj; Xrp1*/+ wing discs. Dots in the graph represent total count of puncta in a wing disc. (statistical test: unpaired t-test for both the quantifications, **** P<0.0001, *** P = 0.0006, SD error bars).

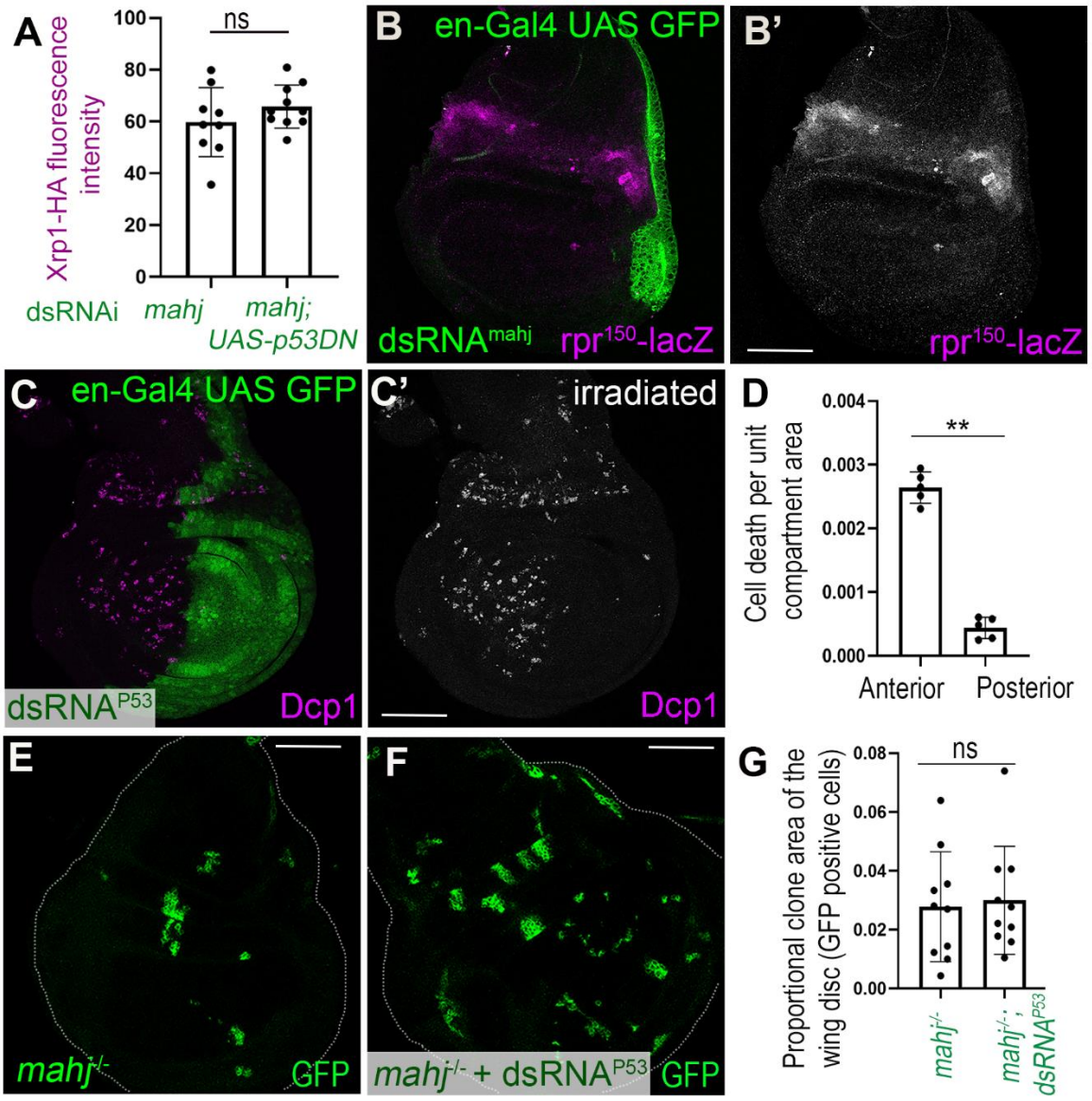

Fig. S3. *mahj* mediated cell competition is independent of *p53*

(A) Quantification of Xrp1-HA fluorescence signal in the posterior compartment of wing discs upon knockdown of *mahj* and one with simultaneous expression of UAS-*p53* DN (Representative images shown in Fig. 3A-B). (B-B') Wing disc with knockdown of *mahj* in posterior compartment (green) and expression of *rpr*-LacZ (magenta, see also B'). LacZ level in posterior compartment was unaffected. N=7. (C-C'') Irradiated wing disc expressing *p53* RNAi in posterior compartment (green) and stained for Anti-Dcp1(magenta, see also C'). Note reduction in cell death in posterior compartment.

N=5. (D) Quantification of irradiation-induced cell after *p53* inhibition. (E-F) Wing discs with *mahj* mutant clones (green). (E) Only small clones survived. n=10. (F) *p53* knockdown did not rescue *mahj* mutant clones (tub-Gal4>p53 RNAi). n=10. (G) Quantification of *mahj* clone size with and without *p53* knockdown. Statistics: Mann-Whitney test for A, D and unpaired t-test for G, ** P= 0.0079, ns = not significant, SD = error bars, Dots in graph represent data from individual wing discs, scale bar: 50 μm.

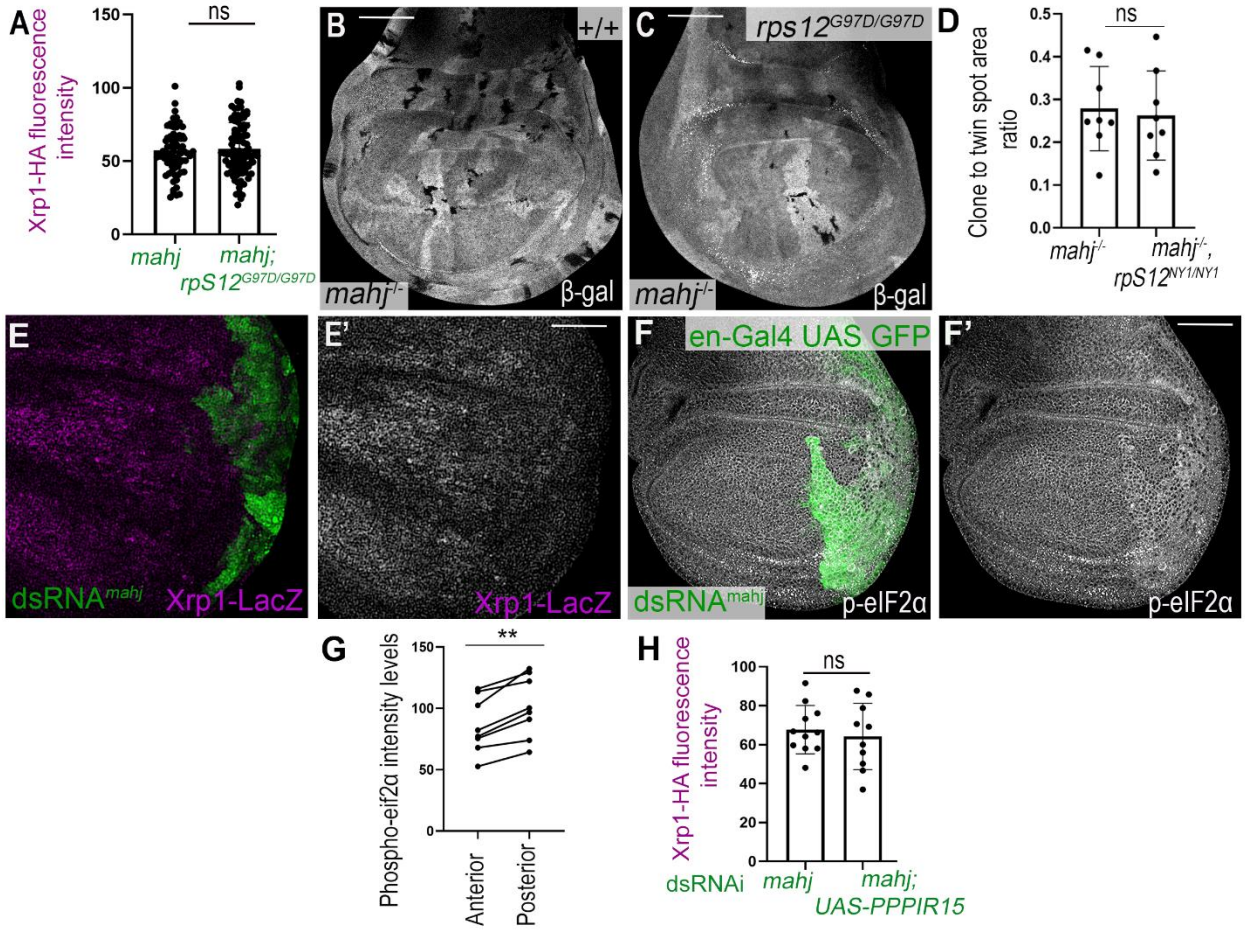

Fig. S4. *mahj* mutant cells express Xrp1 independently of RpS12 and eIF2α phosphorylation

(A) Quantification of experiments shown in Fig. 3C-D, that is, Xrp1-HA fluorescence signal in the *mahj* clones in the wild type and *rpS12*^{G97D} mutant background. Dots in the graph represent Xrp1-HA signal from individual *mahj* clones. (B) *mahj* mutant clones (black) are under-represented in the wild type wing disc compared to reciprocal controls (white). n=8. (C) *mahj* mutant clones (black) are similarly eliminated from *rpS12*$^{G97D/G97D}$ wing discs. n=8. (D) Quantification of *mahj* clone size with respect to twin spot in wild type and *rpS12*^{G97D} mutant background. (E-E') Wing disc with *mahj* knockdown in the posterior compartment (green) and *Xrp1*-LacZ enhancer trap line (magenta, see also E'). Note, *Xrp1*-LacZ expression is unaffected in the posterior

compartment. n=5. (F-F') Wing disc with knockdown of *mahj* in posterior compartment (green) and stained for phospho-eIF2α(gray, see also F'). phospho-eIF2α is higher in posterior compartment. n=8. (G) Quantification of phospho-eIF2α levels upon mahj knockdown in the posterior compartments; anterior compartments of the same wing discs serve as controls. (H) Quantification for Fig 3E, that is of Xrp1-HA fluorescence signal in the posterior compartment of wing discs upon knockdown of *mahj* (n=11) and one with simultaneous expression of UAS-*pppIR15* (n=10). Statistics: unpaired t-test for A & H, Mann-Whitney test for D and Wilcoxon matched-pairs signed rank test for G, ** P= 0.0078, ns = not significant, SD = error bars. Dots in panels D and H represent data from individual wing disc and same hold true for paired dots of panel G. scale bar: 50 µm,

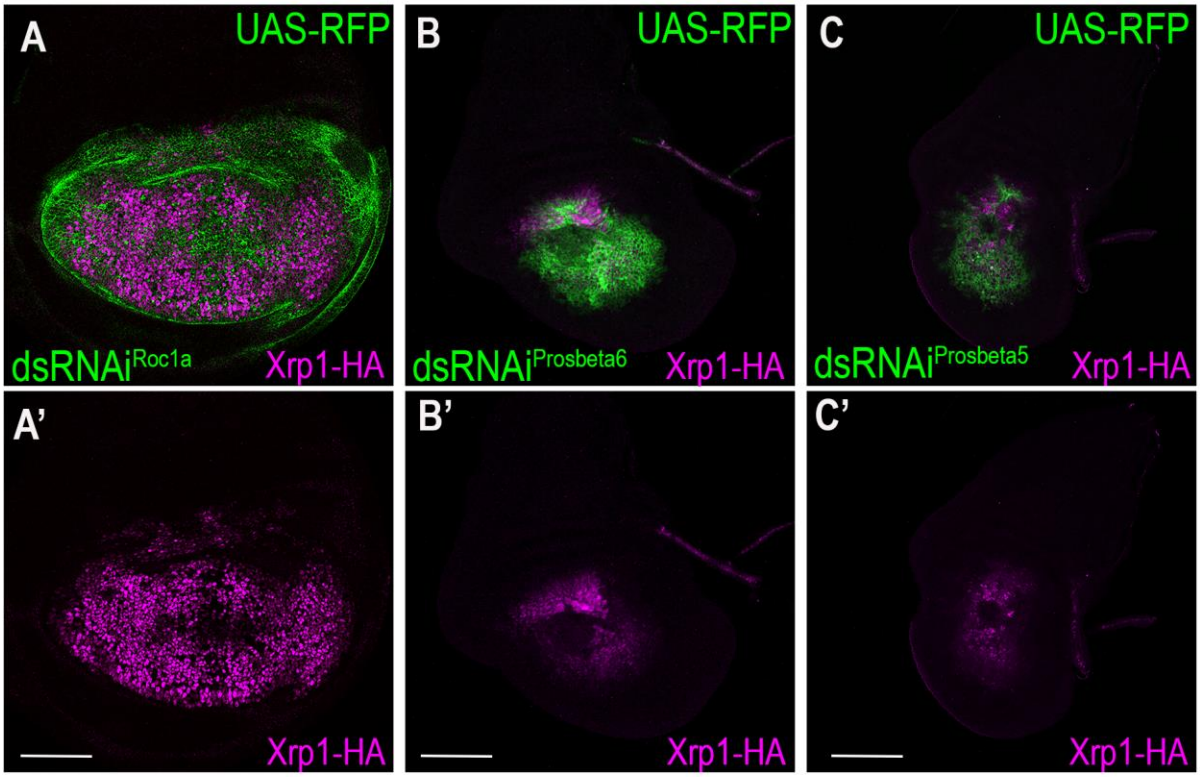

Fig. S5. Xrp1 protein expression in upon knockdown of *Roc1a* or proteasome subunits

(A-C') All panels show wing discs with RFP (green) and the indicated transgenes expressed in the wing pouch domain with nubbin-Gal4. Xrp1-HA expression is in magenta (see also panels A'-C'). (A-A') *Roc1A* knockdown activates Xrp1-HA, n=9. (B-B') Knockdown of proteasome subunit *Prosβ5* activates Xrp1-HA, n=11. (C-C') Knockdown of proteasome subunit *Prosβ6* activates Xrp1-HA, n=12. scale bar: 50 μm

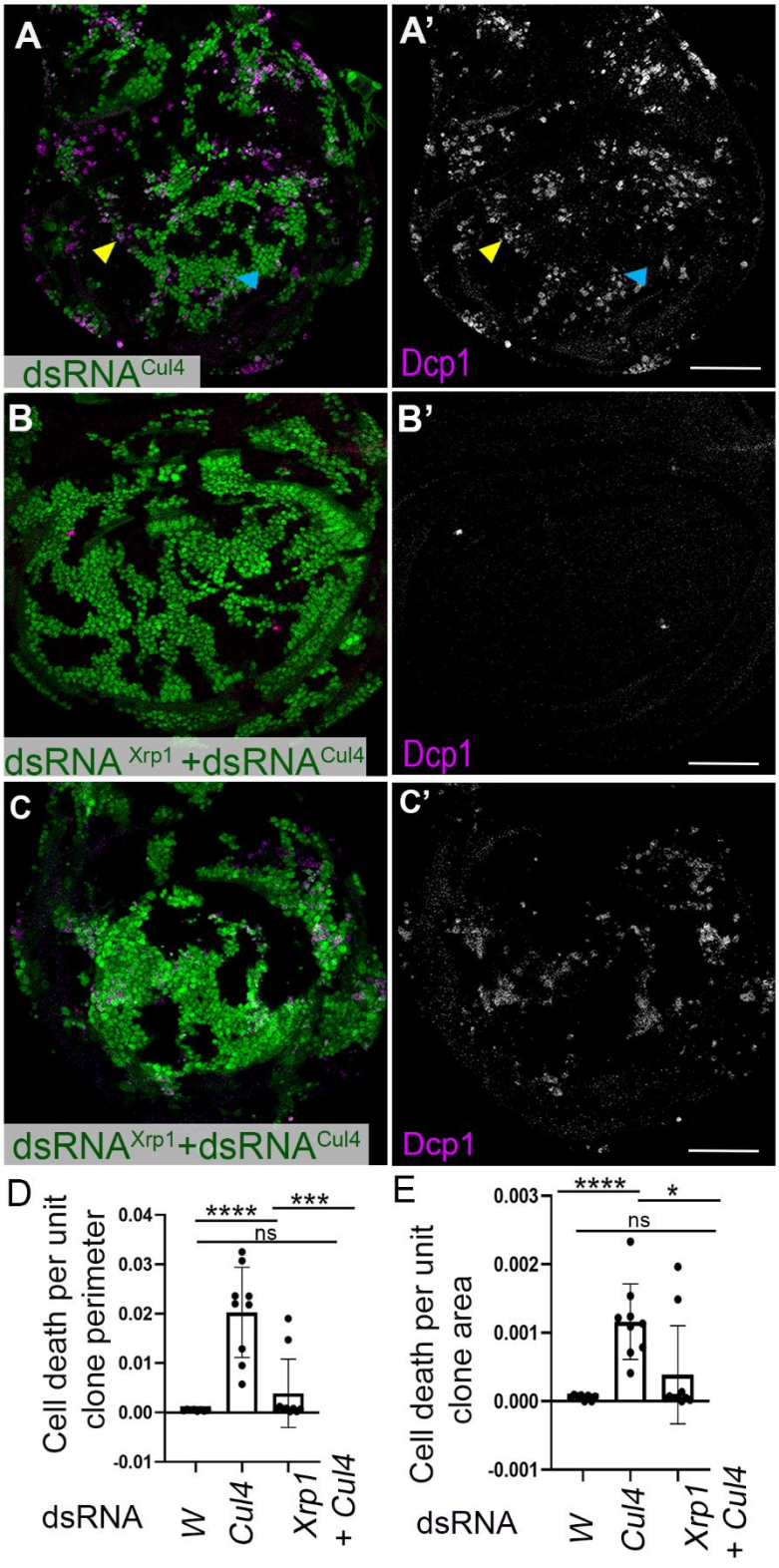

Fig. S6. Cell death upon *cul4* knockdown and its regulation by *Xrp1*

(A-C') Wing disc with flip-out knock-down clones (green) at 48 h showing cell death in magenta. (A) *cul4* knockdown induces cell death (magenta), especially at clone boundaries (see also A', yellow arrowhead) and within clones (cyan arrowhead). n=9 (B) In most cases (8/10), simultaneous *Xrp1* knockdown rescues cell survival in *cul4* knock-down clones (see also B') (C) In some cases (2/10), cell death persisted in *cul4* knock-down clones also depleted for *Xrp1* (see also C'). (D) Quantification of cell death as a function of clone perimeter. (E) Quantification of cell death as a function of clone area. (**** P<0.0001, *** P = 0.0004, ns = not significant, for D and **** P<0.0001, * P = 0.0178, for E, t test, SEM error bars). (Dots in the graph D and E represent data from single wing disc, statistical test used: Mann-Whitney test, **** P<0.0001, *** P= 0.0006, * P= 0.0133, ns = not significant, SD = error bars). scale bar: 50 μm.

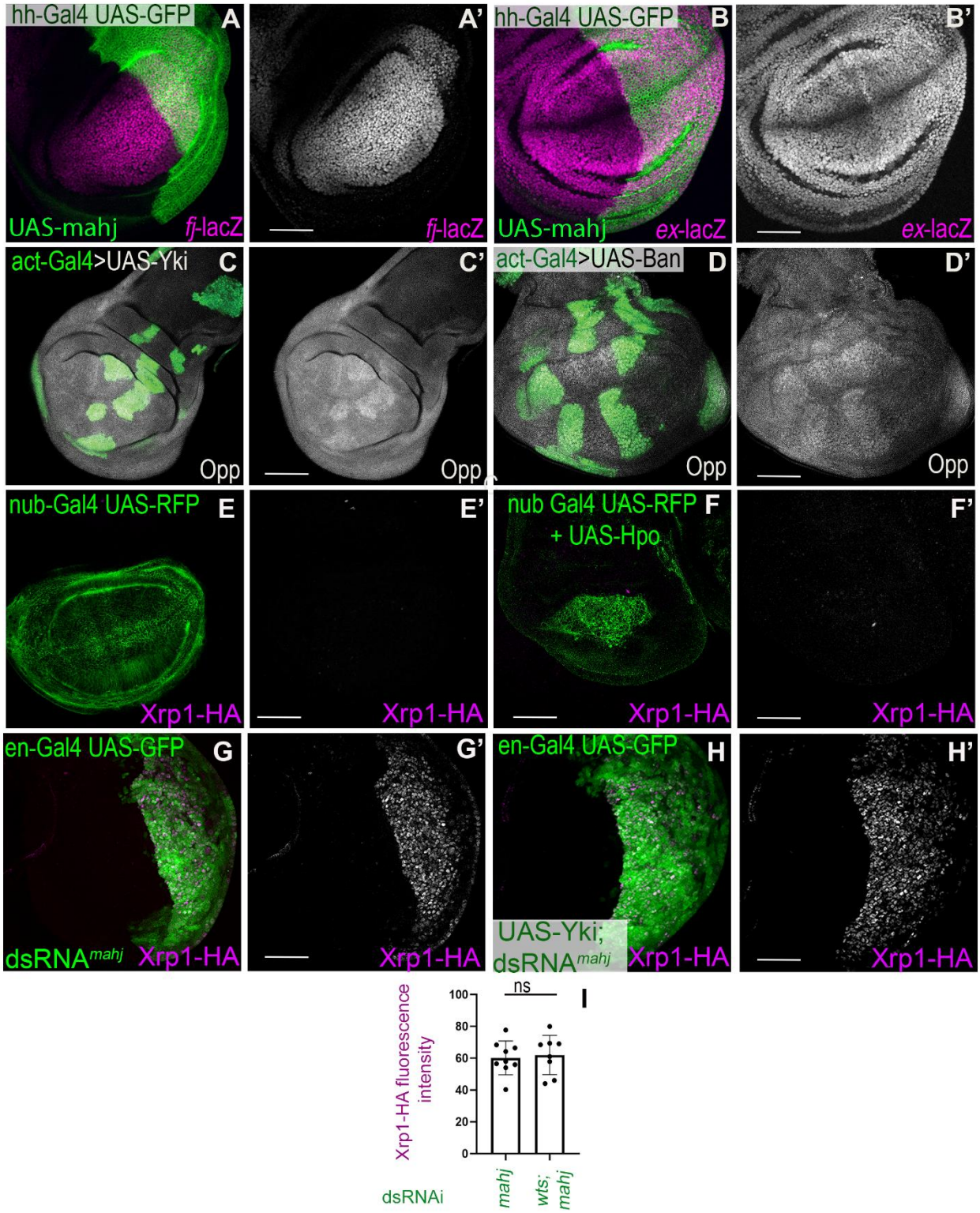

Fig. S7. SWH pathway regulates global translation in the wing disc, but remains dispensable for regulation of Xrp1 expression upon *mahj* knockdown

(A-B') Wing disc with mahj over-expression in the posterior compartment (green) and SWH reporters in magenta. (A) *fj*-LacZ expression remains unchanged upon over-expression of *mahj* (see also A', n=8). (B) *ex*-LacZ expression remains unaffected by overexpression of *mahj* (see also B', n = 10). (C-D) Wing discs with flip-out clones (green) labeled for translation rate (OPP labeling, gray). (C) *yki* over-expression increased global translation rate (see also C', n =6). (D) *ban* over-expression increased global translation rate (see also D', n=8).

(E) Wing disc with pouch domain marked by RFP (green) using *nub*-Gal4 driver did not display Xrp1-HA expression (magenta, see also E', n = 6). (F) *hpo* overexpression using nub-Gal4 did not induce Xrp1-HA expression in the wing pouch (magenta, see also F', n=10). (G) wing disc with *mahj* knockdown using en-Gal4 driver (green) and Xrp1-HA in the posterior compartment (magenta, see also G', n=8). (H-H') Xrp1-HA expression (magenta) continued in posterior compartments depleted for *mahj* and over-expressing *yki* (green, n=8). (I) Quantification of Xrp1-HA upon *mahj* knockdown and one with co-expression of *wts* RNAi. Representative images are shown in Fig 6G-H'. Statistics: Mann-Whitney test, ns = not significant, SD = error bars, dots in the graphs represent data from single wing disc. scale bar: 50 μm.

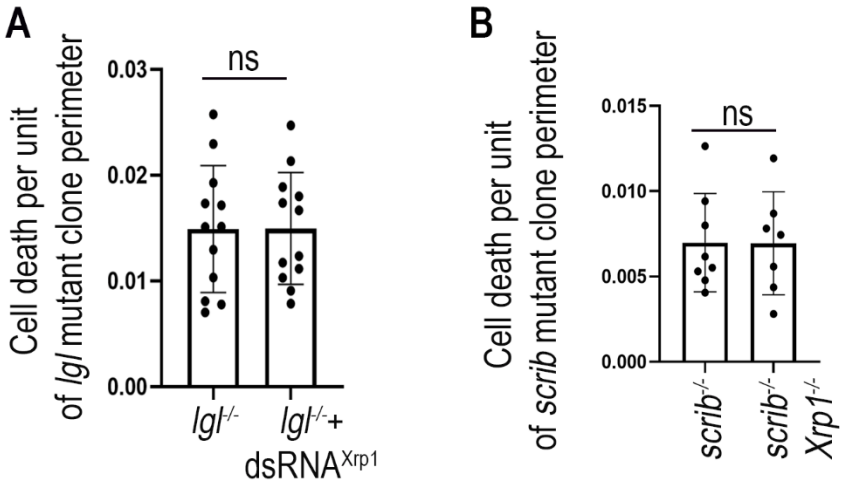

Fig. S8. Quantification of competitive cell death for Fig 7 B-C and Fig. 7 D-E

(A) Quantification of boundary cell death for *lgl* mutant clones and one also depleted for Xrp1. n= 12 for each genotype and samples examined were same as for Fig 7D. (B) Quantification of boundary cell death for *scrib* mutant clone and *scrib Xrp1* double mutant clones. Samples examined were same as for Fig 7G, except that those wing discs from which *scrib* mutant clones were completely eliminated could not be analyzed. n= 7 & 8 for wing disc with *scrib* and *scrib xrp1* double mutant clones, respectively. (Dots in the graphs represent data from single wing disc, unpaired t-test for A and Mann-Whitney test for B, ns = not significant, SD = error bars).